(2)

AD-A206 988 REPORT DOCUMENTATION PAGE

1b. RESTRICTIVE MARKINGS: DTIC FILE COPY

2a. SECURITY CLASSIFICATION AUTHORITY

2b. DECLASSIFICATION / DOWNGRADING SCHEDULE

3. DISTRIBUTION / AVAILABILITY OF REPORT
Approved for public release; distribution unlimmeted

4. PERFORMING ORGANIZATION REPORT NUMBER(S)
Chemical Dynamics Corporation

5. MONITORING ORGANIZATION REPORT NUMBER(S)
AFOSR-TR- 89-0461

6a. NAME OF PERFORMING ORGANIZATION
Chemical Dynamics Corporation

6b. OFFICE SYMBOL (If applicable)

7a. NAME OF MONITORING ORGANIZATION
USAF, AFSC AFOSR /NE

6c. ADDRESS (City, State, and ZIP Code)
9560 Pennsylvania Avenue
Upper Marlboro, Maryland 20772

7b. ADDRESS (City, State, and ZIP Code)
Air Force Office of Scientific Research
Building 410, Bolling AFB,DC 20332-6448

8a. NAME OF FUNDING / SPONSORING ORGANIZATION
USAF,AFSC AFOSR

8b. OFFICE SYMBOL (If applicable)
NE

9. PROCUREMENT INSTRUMENT IDENTIFICATION NUMBER
F49620-88-C-008 6

8c. ADDRESS (City, State, and ZIP Code)
Air Force Office of Scientific Research
Building 410
Bolling AFB,DC 20332-6448

10. SOURCE OF FUNDING NUMBERS

PROGRAM ELEMENT NO.	PROJECT NO.	TASK NO.	WORK UNIT ACCESSION NO.
61102F	3005	A1	

11. TITLE (Include Security Classification)
GROWTH STUDIES OF METAL-METAL/ SEMICONDUCTOR STRUCTURES

12. PERSONAL AUTHOR(S)
C.S. MURTHY, B.M. RICE and M.J. Redmon

13a. TYPE OF REPORT	13b. TIME COVERED	14. DATE OF REPORT (Year, Month, Day)	15. PAGE COUNT
Final	FROM 1AUG88 TO 31Jan89	31MAR89	

16. SUPPLEMENTARY NOTATION THE VIEW, OPINIONS AND/OR FINDINGS CONTAINED IN THIS REPORT ARE THOSE OF THE AUTHORS AND SHOULD NOT BE CONSTRUED AS AN OFFICAL AFOSR POSITION, POLICY, OR DECISION.

17. COSATI CODES		
FIELD	GROUP	SUB-GROUP

18. SUBJECT TERMS (Continue on reverse if necessary and identify by block number)
SEE REVERSE

19. ABSTRACT (Continue on reverse if necessary and identify by block number)

SEE REVERSE

20. DISTRIBUTION / AVAILABILITY OF ABSTRACT
☒ UNCLASSIFIED/UNLIMITED ☐ SAME AS RPT. ☐ DTIC USERS

21. ABSTRACT SECURITY CLASSIFICATION
UNCLASSIFIED

22a. NAME OF RESPONSIBLE INDIVIDUAL
Cole W. Litton

22b. TELEPHONE (Include Area Code)
202-767-6946 4433

22c. OFFICE SYMBOL
AFOSR/NE

DD FORM 1473, 84 MAR 83 APR edition may be used until exhausted. All other editions are obsolete.

SECURITY CLASSIFICATION OF THIS PAGE

89 0 4 18 058

Block 18 - Subject Terms (continued)

Interaction Potential Modelling, Computer Simulation, Embedded Atom Methods, Strain, Positive and Negative Misfit, Axial Commensuration, Adatom Diffusion, Directional Anisotropy

Block 19 - Abstract (continued)

The overall goal of the research program is to develop an atomistic approach to gain an understanding of the mechanisms of growth processes and to contribute to the development of metal/metal and metal/semiconductor heterostructures. The Phase I research involved (i) reliable modelling of underlying atomic interactions within the atomic constituents of the substrate, interface, and adlayer; (ii) static and dynamical studies of interfacial energetics and kinetics. A survey of available modelling schemes has been made and a strategy for our own future modelling efforts is identified. Nickel, Copper. (mgn.)

An analysis of the various modelling schemes for adatom diffusion studies, based on the application of dynamical calculations, has shown that (a) all the models exhibit the experimentally observed directional anisotropy for the self diffusion on Ni (110) surface, (b) estimates of the classical diffusion barrier for Ni/Ni (100), Ni/Ni (110), and Ni/Ni(111) indicates that diffusion will occur more readily on (111) surface orientation, and (b) at high temperatures, the models agree with each other but as temperature decreases the predicted diffusion data fall within a scatterband. The latter observation points out the necessity for precise measurements of self-diffusion of Ni on Ni.

Atomistic static energetics of a Ni monolayer on a Cu substrate, based on both a simple pairwise additive potential and a more realistic many-body potential model, indicate that the characterization of the details of axial commensuration in terms of energy minima and maxima is found to depend on the atomistic model such as rigid vs nonrigid (nonrigid approximation corresponds to the inclusion of adatom-adatom interactions) for the adlayer. A successful determination of the separation of the total adatom-substrate interaction energy in the realistic model led to energy charactersitics, within the rigid lattice approximation, that are similar to those obtained with the simple pairwise potentials. This implies that for rigid lattices the energetics are only determined by the relative atomic sizes of the substrate and monolayer.

The strain energy for Cu/Ni is larger than that of Ni/Cu. This indicates that a large number of layers will grow pseudomorphically in the case of negative misfit interface, Ni/Cu. Studies involving the adatom diffusion and the strain energy dependence on the substrate orientation may provide a clue to the choice of substrate orientation for obtaining better quality films and for understanding the competition between energetics and kinetics at various temperatures.

OBJECTIVES

Introduction

An atomistic understanding of the metal-metal and metal-semiconductor interfaces is highly desirable, both for fundamental physical reasons and due to increasingly sophisticated technical applications. Both stable and metastable phases through the growth of epitaxial thin films on suitable substrates have been observed recently [1] and are leading to the fabrication of superlattices. Although many of the growth parameters are controllable in the modern molecular beam epitaxy (MBE) and metalorganic chemical-vapor deposition (MOCVD) techniques,[2,3] the precise roles of not only the various growth parameters but also of the energetics and kinetics in affecting the diverse phenomena occurring at growth fronts are not known. Furthermore, sometimes the precise interpretation of the nature of growth becomes difficult. For instance, there is some controversy in the recent literature[4] regarding epitaxial fcc Fe films on Cu (100). A microscopic approach via dynamical simulations for such issues would play a dominant role in clarifying this controversy of the heterostructure in terms of the energetics, structure and kinetics of the atoms involved.

Although there have been a few atomistic energetic studies,[5] these studies have been based on the Lennard-Jones form for atomic interactions which is inadequate for metallic and semiconductor modelling. These preliminary level calculations, however, provided a clue on the strains which could be developed in the deposited layer due to the lattice mismatch. As realistic interaction potentials are being produced for metals[6] and semiconductors,[7] it is timely that quantitative information concerning growth and interface be obtained by adapting these potentials in computer simulations. The recent intense studies on homoepitaxial growth of Si[8] have addressed a number of interesting issues: (a) the growth dependence on the surface orientation, (b) growth characteristics as a function of temperature, (c) significance of annealing after deposition (d) the role of atomic collisions, (e) atom versus cluster deposition and (f) growth mode. These studies are not only model-based but also do not take into account the electronic structural features.

First principles energy-band calculations[9] are being performed on these new materials but they do not include finite temperature effects. An hybrid of computer simulations and electronic structure calculations to do away with model potentials would be most ideal but they are in their infancy[10] because computationally such an approach is so numerically intensive that presently it is restricted to very short simulated times and small number of atoms. For an aggregate of even a few hundred atoms, the only feasible study today is computer simulations based on model potentials. It is therefore important to contrast the results of effective potentials to these first-principle type calculations.

The overall goal of the proposed research is to develop an atomistic approach to gain an understanding of the mechanisms of processes to fabricate metal-metal/semiconductor structures and thus to contribute to their development. The complexity of the approach involving realistic modelling of atomic interactions and adaption/development of a suitable dynamical simulation technique or hybridized techniques can be broken down into its component parts which can be studied stage by stage and and can be grouped. The primary goal in Phase I was to systematically obtain the energetics and structural features of the interfaces of Cu/Fe and to simulate the dynamical processes occurring during growth.

Phase I Rcsearch Objectives

The specific objectives of Phase I follow:

- The development of realistic interaction potentials to describe interatomic interactions. Devise functional forms which are physically motivated and can be par~meterized to experimental data. One test of the usefulness of this approach is to fit the potential to a set of experimental / empirical data and verify that it can be used to predictively extend these results to other experiment conditions.
- The examination of energy characteristics of the heterostructure. Conduct energetics studies of adsorbate-substrate structure using the derived interaction potentials. Examine strain energy for lattice mismatched systems. A comparison of the results between the static and dynamic simulations will address the important question of atomic relaxation and anharmonic effects.
- The identification of key kinetic parameters controlling the growth process of thin films of a few layers. Simulate the dynamical processes occurring during growth.

Towards this end, Phase I laid the groundwork by delving into the microscopic energetics and adatom diffusion studies, dynamics of representative processes important in the epitaxial and superlattice growth phenomena. We proposed to examine the Fe/Cu structure. Although this structure is being studied intensely[1,4] due to the novel magnetic properties of the formed films, the emphasis and the above discussed experimental controversy is on fcc Fe/Cu as opposed to bcc Fe/Cu. Modelling of an hypothetical fcc Fe would not be realistic because most of the bulk data is for bcc Fe. It was also felt that potential model -based investigations (that too for an hypothetical structure) may not contribute effectively to resolve the experimental controversy. Based on these observations and on the discussions we had with the program manager at the time of Phase I research initiation, we chose to investigate the Cu/Ni as a prototype structure.

The rationale for the choice of Cu/Ni is many fold: (a) agreement between experimental investigations,[1,11] (b) lack of detailed growth simulation studies (the predicted critical thickness

based on a Monte Carlo simulation study[12] contradicts with the experiment[11]), (c) availability of four different tested potential models for the bulk metals, Cu and Ni, and (d) opportunity to examine (1) the effects of potential models and (2) the merits and demerits of the different modelling schemes.

RESEARCH STATUS

Interaction Potential Modelling

Computer simulations based on atomistic descriptions of the structure and properties of materials require as input simple yet realistic interaction potentials. They should produce acceptably accurate structural features and energetics with a reasonable expenditure of computer resources. Although most computer modelling studies to date[13] have employed only pairwise additive potentials, many-body interactions and directionally nonisotropic potentials are essential for the description of atomic clusters, interfaces, and strained lattices. The two-body potentials are not suitable for describing metals/semiconductors.

There are two general approaches that can be used for obtaining potentials for application in computer simulation studies. The first employs the methods of quantum chemistry for a first principles (*ab initio*) calculation on a small group of atoms (a cluster) or local density functional (LDF) calculation of the bulk solid. The second approach involves fitting parameters in a physically motivated function to relatively limited experimental data supplemented by results of *ab initio* cluster and/or local pseudopotential calculations. Because of cost, *ab initio* methods are usually not utilized to obtain complete potential energy hypersurfaces. However, data for different cluster geometries and/or adsorbed atom configurations can be used to parameterize empirical potential models and can augment often scarce empirical data.

The embedded atom method (EAM)[14] was developed as a means of calculating realistic ground-state properties of metallic systems. We are drawn to EAM, because of its strong foundation in density functional theory via the effective medium approach. The total energy is simply written as:

$$E_{tot} = \sum_i F_i(\rho_i) + \frac{1}{2} \sum_{ij,\, i<j} \varphi_{ij}(R_{ij}) \qquad (1)$$

where $F_i(\rho_i)$ is the energy needed to embed atom i into the local electron density, ρ_i, of the surrounding atoms, and ϕ_{ij} is a pair potential between atoms i and j.

Different schemes[15] have been used to describe the local electron density and the pair interactions of Eq. (1) for the metals Cu and Ni. The differences between the various approaches are primarily found in the derivation and interpretation of the embedding density of the electron surrounding the atom, ρ, and the embedding function $F(\rho)$. Ackland et al[15d] following Finnis

and Sinclair[14b] used a square-root function for F(ρ) and identified F(ρ) with the second moment of the density of states. Whereas the scheme of Baskes and coworkers scheme (FBD)[15a] is to specify ρ as an atomic charge density obtained from Hartree-Fock calculations for the free atom and then to obtain F(ρ) by empirical fitting to the equation of state of the bulk. Oh and Johnson's approach was to develop an EAM model with simple functional forms which result in less number of parameters to fit and thus provide easy access to the EAM model on any type of the computer.

The evaluation of these schemes in terms of how the models perform in calculation of unfitted properties, such as diffusion, which are appropriate for the planned interfacial and growth studies is discussed below under the accomplishments section in conjunction with the kinetics. However, we feel that the EAM method offers a theoretical framework that holds promise for the development of potentials with improved transferability from bulk simulations to crystal growth and even cluster chemistry. The trick is of course to have a very flexible parameterization scheme for the density, or embedding term F. Our studies of the methodology leads us to the belief that parameterization of the density using only bulk data will not produce an EAM method that is completely satisfactory for studying growth processes. However, by using results of quantum mechanical calculations on clusters in addition to bulk data, even if only of qualitative accuracy, more generally useful densities can be obtained that will satisfy the demands of simulations of growth phenomena. This work must be deferred until Phase II due to time constraints.

Energetics Studies

From a knowledge of the interaction potential of the metallic system under consideration, the total energies of interfaces (composed of the structure with specific surface orientations that differ only in symmetry) are obtained as a function of the lattice constant ratio, relative orientation, and relative displacement between the adsorbate and substrate. These basic variables can be defined in terms of the crystallographic relationships[5c] between the two structures considered. The substrate model remains fixed. The variation of energy as a function of the above variables and their values at the energy minimum give information on the conditions necessary to obtain a coherent interface.

In order to consider the strain effects due to lattice-mismatch at the interface, the strain at the interface can be defined as Strain (%) = $(b - a_a)/a_a$, where b is the strained lattice constant (varying lattice constant in the calculation) and a_a is the unstrained (corresponding to the bulk value) lattice constant of the adsorbate. The total energy of the interface was calculated as a function of the strain (varying adlayer lattice constant). The energy curve shows a minimum with respect to strain, which is dependent on the number of atoms in the adlayer.

A preliminary manuscript of a publication arising from our Phase I research on static energetics with simple pairwise additive potentials and the realistic EAM-based FBD model has

been enclosed as an appendix-1 to this report and presents and discusses our results in detail. The results on the energetics are discussed briefly under the accomplishments section below. We tried to address, in a limited effort due to the time constraints, the important question of atomic relaxation. These studies follow.

Atomic Relaxation Effects

A series of calculations have been carried out in order to examine the effects of atomic relaxation at the dissimilar interface Cu (111)/Ni(100). Details of individual runs are described below. The Ni substrate has 4 layers with 289 atoms in each layer. The Cu adlayer is initially a monolayer.

Run 1: Cu adlayer has 25 atoms and all the atoms are allowed to relax. The 25 first layer Ni atoms closest to the Cu atoms are allowed to relax. All other substrate atoms were held fixed at bulk equilibrium positions.

Run 2: Cu adlayer has 25 atoms and all the atoms are allowed to relax. The 121 Ni atoms each of the first and second layers of the substrate are allowed to relax.

Run 3: 81 Cu atoms in adlayer; all are allowed to move. The 242 Ni atoms in the substrate are allowed to move (121 in each of the first and second layers of substrate) as in run 2. The initial adlayer is positioned directly over the second layer Ni atoms at a distance of 1.805 Å above the surface layer; the lattice constant of the adlayer is initially 3.61 Å.

Run 4: Same crystal model as Run 3 except initial adlayer has lattice constant of 3.52 Å (rather than 3.61 Å) and is located above the surface at a distance of 1.76 Å (rather than of 1.805 Å).

Results: It is clear from a comparison of the values of the bond length and the interplanar distances reported in table1 that in Runs 1 and 2, the Cu adlayer becomes pseudomorphic to Ni. In Run 3, the initial adlayer "breaks up" into small clusters, each little cluster, consisting of approximately 20 atoms, is pseudomorphic to Ni substrate. Whereas in Run 4, some of the atoms in the Cu monolayer migrated to a lattice position above the monolayer; the end result is a pseudomorphic bi-layer of adatoms. These preliminary results that small clusters of an adlayer (~ 25 atoms) will readily form a defect-free monolayer on the substrate. Large clusters, however, do not; the "break up" into small clusters or form new layers, and possibly this is to relieve the strain of the larger cluster.

Material:	Cu	Ni	Cu adlayer*	
			Run 1	Run2
Bond length (Å):	2.556	2.489	2.487	2.490
Interplanar Distance (Å):	1.805	1.76	1.754	1.744

* In Run 1 for the Ni substrate, $< z_{12} > = \Delta d_{12} = -0.00778$ Å. Whereas in Run 2, Ni first layer $\Delta d_{12} = -0.000043$ and for Ni second layer, $\Delta d_{23} = -0.001$ Å

Adatom Diffusion Studies

A knowledge of the mobility of an atom on the surface would aid in for assessing and/or interpreting the order (full vs partial) of epitaxial growth for different surface orientations. The adatom diffusion studies are also useful for evaluation of the potential model provided reliable experimental data is available for comparison purposes with theoretically predicted values. Instead of adapting the cost-intensive molecular dynamical simulations for estimating the diffusion constants, we used the variational transition state theory approach to compute Arrhenius parameters and diffusion coefficients. Appendix-2 to this report, as a preliminary manuscript of a publication arising from these studies, describes and discusses our results on the self-diffusion of Ni for four different EAM-based model potentials. The observed sensitivity of the variation of diffusion to the interaction potential parameters and comparison with experiment are discussed below.

Accomplishments

Potential Model Evaluations and Self-Diffusion

Analysis of various embedded-atom type modelling schemes for adatom diffusion studies, to our knowledge, represents the first study based on the realistic bulk models. For an unbiased evaluation of EAM models used, a stringent comparison with experiment is difficult due to (a) the lack of a quantitative relationship between the intrinsic (corresponding to an ideal flat surface) and mass transfer (involving the complex processes of the formation of surface defects and their migration) surface diffusion data as a function of temperature, the former being consistent with the calculations, and (b) the existence of contradictory data for the difference in the measured intrinsic and mass transfer data as well as large scatter in the experimental data. We find that

- All the models exhibit the directional anisotropy for the self diffusion on Ni (110) surface.
- At high temperatures, the models agree with each other but as temperature decreases the predicted diffusion data fall within a scatterband.
- Comparison of the classical diffusion barrier for Ni/Ni (100), Ni/Ni (110), and Ni/Ni(111) indicates that diffusion will occur more readily on (111) surface orientation. This may imply that the homoepitaxial growth will be relatively complete for (111) substrate orientation. This is borne out in a recent molecular dynamics simulation[16] of homoepitaxial growth using Lennard-Jones model.

These studies involving the surface diffusivity and surface structure with realistic interaction potentials as well as the explosive developments in the growth techniques should result in renewed impetus for accurate measurements of adatom diffusion.

Energetics

Atomistic studies on static energetics of Ni monolayer growth on the Cu substrate have been performed using both central potentials and the realistic EAM-based FBD model. We find that

- The characterization of the details of axial commensuration in terms of energy minima and maxima is found to depend on the atomistic model (rigid vs nonrigid, nonrigid approximation corresponds to the inclusion of adatom-adatom interactions) for the adlayer
- Upon successful determination of the embedding energy contribution to the total adatom-substrate interaction energy, the energy charactersitics turned out to be similar to those obtained in the recent detailed studies with simple model potentials. This implies that for rigid lattices the energetics are only determined by the relative atomic sizes of the substrate and monolayer.
- The strain energy for the positive misfit interface (Cu/Ni) is larger than that of the negative misfit interface (Ni/Cu). This implies that a large number of layers will grow pseudomorphically in the case of negative misfit interface. This type of estimate is of great interest in the fabrication of superlattices made up of lattice mismatched materials. The diffusion and the strain energy dependence on the substrate orientation may provide a clue to the choice of substrate orientation for obtaining better quality films.
- The preliminary results based on the inclusion of atomic relaxations indicate that the initial adlayer breaks up into small clusters, and each cluster, consisting of approximately 20 atoms, is pseudomorphic to the Ni substrate.

Acknowledgement

This work was supported by the Air Force Officers Scientific Research under grant number F49620-88-C-0086. It is a pleasure to acknowledge useful discussions with Dr. Bruce Garrett regarding the separation of reasonably realistic contribution from the embedding energy to the total adatom-substrate interaction energy. We acknowledge San Diego Supercomputer Center for a reasonable support of supercomputer time at their facility.

References

1 (a) P. A. Montano, Y. C. Lee, J. Marcano, and H. Min, in Layered Structures and Epitaxy, MRS Symposia Proceedings, Vol. 56, ed. J. Gibson, G. C. Osbourne, and R. M. Tromp, (MRS, Pittsburgh, PA 1986), p. 183 and references therein; (b) Z. Q. Wang, S. H. Lu, Y. S. Li, F. Jona, and P. M. Marcus, Phys. Rev. **B35**, 17 (1987); (c) B. Heinrich, K. B. Urquhart, J. R. Dutcher, S. T. Purcell, J. F. Cochran, anf A. S. Arrott, J. Appl. Phys. **63**, 3863 (1988); (d) D. A. Steigerwald, I. Jacob, and W. F. Egelhoff, Jr. Surf. Sci. (1989); (d) S. A. Chambers, T. J. WAgener, and J. H. Weaver, Phys. Rev. B **36**, 8992 (1987).

2 K.Ploog, in Crystals: Growth, Properties and Applications, ed. by H. C.Freyhardt, Vol. 3, p. 73 (Springer, N. Y., 1980).

3 Ch. 2, 5, 8, and 9, in Epitaxial Growth , ed. by J. W. Mathews (Academic, N. Y., 1975).

4 (a) D. A. Steigerwald and W. F. Eglehoff, Jr, Phys. Rev. Lett. **60**, 2558 (1988); (b) D. Pescia, M. Stampanoni, G. L. Bona, A. Vaterlaus, F. Meier, G. Jennings, and R. F. Willis, Phys. Rev. Lett. **60**, 2559 (1988).

5 (a) G. J. Dienes, K. Sieradzki, A. Paskin, and B. Massoumzadeh, Surf. Sci. **144**, 273 (1984); (b) R.Ramirez, A. Rahman, and I. K. Schuller, Phys.Rev. **B30**, 6208 (1985); (c) A. Kobayashi and S. Das Sarma, Phys. Rev. **B35**, 8042 (1987); (d) E. Bauer and J. H. van der Merwe, Phys. Rev. **B33**, 3657 (1986).

6 (a) M. S. Daw and M.I. Baskes, Phys. Rev. **B29**, 6443 (1984);(b) A. F. Voter and S. P. Chen, MRS proceedings, Winter 1986, Symposium I; (c) K. W. Jacobsen, J. K. Norskov, and M. J. Puska, Phys. Rev. B35, 7423 (1987).

7 (a) F. H. Stillinger and T. A. Weber, Phys. Rev. **B31**, 5262 (1985); (b) K. Ding and H. C. Andersen, Phys. Rev. **B34**, 6987 (1986); (c) R. Biswas and D. R. Hamann, Phys. Rev. Lett. **55**, 2001 (1985) and Phys. Rev. B36, 6434 (1987); (d) J. Tersoff, Phys. Rev. Lett. **56**, 632 (1986); (e) B. W. Dodson, Phys. Rev. **B33**, 7361 (1986); ibid. **35**, 2795 (1987); (i) M. I. Baskes Phys. Rev. Lett. **59**, 2666 (1987).

8 (a) M. Schneider, I. K. Schuller, and A. Rahman, Phys. Rev. **B36**, 1340 (1987); (b) B. W. Dodson, **B36**, 1068 (1987); (c) E. T. Gawlinski and J. D. Gunton, Phys. Rev. B36, 4774 (1987); (d) R. Biswas, G. S. Grest, C. M. Soukoulis, Phys. Rev. B38, 8154 (1988); (e) J. Lampinen, R. M. Nieminen, and K. Kaski, Surf. Sci. **203**, 201 (1988); (f) M. H. Grabow and G. H. Gilmer, Surf. Sci. **194**, 333 (1988); (g) W. Lowell Morgan, in "MD Simulation of the Physics of Thin Film Growth of Si: Effects of the Properties of Interatomic Potential Models" in Atomistic Modelling of Materials: Beyond Pair Potentials ed. V. Vitek and D. J. Srolovitz , (Plenum to be published) World Materials Congress Proc. 1988.

9 (a) V. L. Moruzzi, P. M. Marcus, K. Schwarz, and P. Mohn, Phys. Rev. B34, 1784 (1986); (b) P. M. Marcus, V. L. Moruzzi, Z. Q. Wang, Y. S. Li, and F. Jona, in Physical and Chemical Properties of Thin Metal Overlayers and Alloy Surfaces, MRS Symposia Proceedings, Vol. 83, ed. D. M. Zehner and D. W. Goodman (MRS, Pittsburgh, PA, 1987); (c) R. E. Watson, M. Weinert, and J. W. Davenport, Phys. Rev. B35, 9284 (1987); (d) G. P. Srivastava and D. Weaire, Adv. Phys. **36**, 463 (1987) and references therein.

10 (a) R. Car and M. Parrinello, Phys. Rev. Lett. **55**, 2471(1985); (b) O. F. Snakey and R. E. Allen Phys. Rev. **B33**, 7164 (1986); (c) M. Menon and R. E. Allen, Phys. Rev. **B33**,7099 (1986); (d) M. Needles, M. C. Payne, and J. D. Joannopoulos, Phys. Rev. Lett. **58**, 1765 (1987).

11 (a) A. Chambers and D. C. Jackson, Phil. Mag. **31**, 1357 (1975); (b) S. A. Chambers, H. W. Chen, I. W. Vitomirov, S. B. Anderson, and J. H. Weaver, Phys. Rev. **B33**, 8810 (1986).

12 B. W. Dodson, Surf. Sci. **184**, 1 (1987).

13 (a) C. S. Murthy, K. Singer, and I. R. McDonald, in Molecular Based Study of Fluids, ed. by J. M. Haile and G. A. Mansoori, p. 189 (ACS, Washington, D. C., 1983);.(b) C. S. N. Murthy and M. Dixon, Phys. Chem. Liquids **12**, 83 (1982); (c) See an execellent recent review by R. A. Johnson, in "Computer Simulation in Materials Science" ed. R. J. Arsenault, J. Beeler, and D. M. Esterling (ASM 1988); (d) See various papers in Interatomic Potentials and Crystalline Defects, ed. J. K. Lee (Metallurgical Society of AIME, New York 1981).

14 (a) M. S. Daw and M. I. Baskes, Phys. Rev. Lett **50**, 1285 (1983); M. S. Daw and M. I. Baskes, Phys. Rev. B **29**, 6443 (1984); (b) M. W. Finnis and J. E. Sinclair, Phil. Mag. A **50**, 45 (1984).

15 (a) S. M. Foiles, M. I. Baskes, and M. S. Daw, Phys. Rev. B **33**, 7983 (1986); (b) A. F. Voter and S. P. Chen, Mater. Res. Soc. Symp.**82**, 175 (1987); (c) D. J. Oh and R. A. Johnson, J. Mater. Res. **3**, 471 (1988) and " Embedded Atom Method for Close-Packed Metals "Atomistic Modelling of Materials: Beyond Pair Potentials" ed. V. Vitek and D. J. Srolovitz , (Plenum to be published) World Materials Congress Proc. 1988; (d) G. J. Ackland, G. Tichy, V. Vitek, and M. W. Finnis, Phil. Mag. **56**, 735 (1987).

16 S. M. Paik and S. Das Sarma, Phys. Rev. B **39**, 1224 (1989).

LIST OF PUBLICATIONS

The following manuscripts resulted from research supported under the present Phase I contract and are included as appendices to this report.

(1) "Embedded-atom Type Energetics for FCC Metallic Interfaces", C. S. Murthy and B. M. Rice, Bull. Amer. Phys. Soc. 34, No. 3, 545 (1989), (for publication in Phys. Rev. B).

(2) "Comparative Study of Embedded-atom-Method (EAM) Potentials: Self-diffusion on FCC Metallic Surfaces", B. M. Rice, C. S. Murthy, , M. J. Redmon, and B. C. Garrett, Bull. Amer. Phys. Soc. 34, No. 3, 545 (1989) (to be submitted to Surf. Sci.).

PERSONNEL

Drs. C. S. Murthy, B. M. Rice, and M. J. Redmon were supported by this contract.

APPENDIX-1

Embedded-Atom Type Energetics for FCC Metallic Interfaces

Preliminary Version

Embedded-Atom Type Energetics for FCC Metallic Interfaces

C. S. Murthy and B. M. Rice
Chemical Dynamics Corporation*
Upper Marlboro, MD 20772

* Mailing Address: 9560 Pennsylvania Avenue, Suite 106, Upper Marlboro, MD 20772

Abstract

Atomistic studies on static energetics of Cu monolayer growth on a Ni substrate are presented. The sensitivity of the characteristics of the energetics, as a function of the ratio of the lattice constants, to the chosen atomistic model such as rigid versus nonrigid (nonrigid approximation corresponds to the inclusion of adatom-adatom interactions) for the adlayer and the interaction potential is discussed. Conditions necessary to obtain a coherent interface between fcc(111)/fcc(100) structures are then examined in terms of axial commensuration. The strains and the strain energies at interfaces which exhibit either positive misfit [Cu/Ni(100)] or negative misfit [Ni/Cu(100)] are obtained employing the recently developed embedded-atom potentials for Ni and Cu.

I. INTRODUCTION

Extensive experimental work has been carried out to study the growth of semiconductors and metals on a variety of substrates,[1] and the growth of semiconducting[2] and metallic superlattices.[3] Theoretical work, until recently, has mainly focussed on thermodynamics and kinetics of crystal growth. An atomic scale understanding of crystal growth is required to predict novel material properties and for device applications. A direct brute-force microscopic approach would lead to a detailed understanding of the interface formation. Rigid lattice model calculations of energetics, starting with the pioneering work of Frank and van der Merwe,[4] have dealt with studies of growth patterns,[5] effect of substrate induced strains on the orientation of monolayer adsorbates.[6] The advent of supercomputers has however made it possible to undertake detailed static energetics studies.[7]

The recent detailed atomistic static energetic studies[7b] have explored the dependence of interface formation on lattice-constant ratio, relative orientation, and relative displacement between the substrate crystal and the formed film and the conditions for interface coherency of two dissimilar structures such as fcc (111)/bcc (110), fcc (111)/fcc (100), and fcc (111)/fcc (110). These studies are based on rigid lattice approximation with pairwise additive potentials. That is to say only the adsorbate-substrate (a-s) interactions have been considered in calculating energy versus the lattice mismatch parameter, P defined as a_a/a_s. The values of P pertaining to the minima and maxima in the configurational energy, U_{a-s} has been interpreted in terms of axial commensuration for these dissimilar structures.

In the calculation of energy versus P, the substrate model remains fixed during the calculation (in other words, the lattice constant of the substrate does not change); therefore, the geometries of the substrate atoms do not change. However, the monolayer adsorbate is changed during the calculation; as P is increased, the lattice constant of the adlayer increases and thus geometries of the adsorbate atoms change. Thus, the total energy of the interface corresponds to a sum of U_{a-s} and U_{a-a} where U_{a-a} is configurational energy of the adsorbate-adsorbate interaction. Therefore, while there may exist a P which shows energy minima and maxima characteristics, the role of including U_{a-a} interactions and the effects of atomic relaxations have not been examined until now. The results of the latter studies will be discussed in a forthcoming publication. Under such realistic situations, it would be interesting to see if, in fact, the most stable configuration occurs when axial commensuration is attained.

As realistic interaction potentials are being produced for metals[8] and semiconductors,[9] it is timely that quantitative information concerning growth and interface be obtained by adapting these potentials in computer simulations. Further, it is hoped that this quantitative information on energetics can be compared to first-principles-total-energy calculations which are increasingly becoming available.[10] We have undertaken such a study with realistic potentials, based on the

embedded atom method (EAM), for Cu and Ni metallic structures and the static energetics are considered in this paper. The preliminary results based on the inclusion of atomic relaxations reported elsewhere[11] indicate that the initial adlayer breaks up into small clusters, each cluster, consisting of approximately 20 atoms, is pseudomorphic to the Ni substrate.

The remainder of the paper is organized as follows. Section 2 provides the computational details which includes the lattice models of the substrate and adlayer structures used in the calculations and description of the EAM potential used in this study. The results of the energetics and of the strain and strain energy for lattice mismatched interfaces are reported and discussed in section 3. Concluding remarks are given in Section 4.

II. COMPUTATIONAL DETAILS

Lattice Models:

The lattice models for the calculations using simple model pairwise additive potentials are the same as the one used in previous energetics studies[7b] for obtaining the conditions necessary to obtain a coherent interface between two dissimilar structures. The hexagonal-shaped adlayer was constructed in such a way that it represents the first island formation before interactions with other islands take place. The substrate consisted of 441 atoms per monolayer with a total 3 monolayers stacked normal to the growth axis and the top layer forms a two-dimensional fcc(100) face with a rhombic unit cell. The fcc (111) type adlayer constitutes 121 atoms on rhombic mesh. The coordinates of the central atom of the hexagonal-shaped adlayer is placed directly on the top of the center of the substrate surface. As one is interested in investigating the differences of the results between simple model potentials and realistic EAM potential models models, we have not considered other three relative displacements studied earlier (see fig.1 of ref.7b). In the case of the calculations with EAM model, the substrate contained 289 atoms per layer with three layers altogether and the adlayer is of 121 atoms.

For obtaining the strain and strain energetics at Cu/Ni and Ni/Cu interfaces, the substrate consisting of 289 atoms per layer with three such layers and the (100) orientation and the adlayer with (100) orientation has been constructed. The data has been obtained for four different values of the adsorbate atoms: N_a=25, 49, 81, and 121.

Interaction Potential Models:

In the embedded atom method the configurational energy of a collection of atoms is expressed as a sum of a density-dependent embedding energy and a pair interaction term:

$$U = \sum_i F_i(\rho_i) + \frac{1}{2}\sum_{i \neq j} \phi_{ij}(r_{ij}) \qquad (1)$$

where $F_i(\rho_i)$ is the energy needed to embed atom i into the local electron density, ρ_i, of the surrounding atoms, and ϕ_{ij} is a pair potential between atoms i and j. Different schemes have been used to describe the local electron density and the pair interactions of Eq. (2).

The EAM was developed as a means of calculating realistic ground-state properties of metallic systems. Its success in predicting a wide variety of phenomena in metallic systems, coupled with its low computational demands, makes it a highly desirable alternative to the commonly used and often inadequate pairwise potentials in describing metallic systems. In the approach of Foiles, Daw and Baskes (FBD)[12] which is adopted in the present studies, the local electron density ρ_i into which atom i is embedded is approximated by the sum over atomic electron densities $\rho_j^a(r_{ij})$ from all other atoms in the system:

$$\rho_i = \sum_{i \neq j} \rho_j^a(r_{ij}) \tag{2}$$

This functional form has the advantage of including many-body interactions due to the non-linear nature of the embedding function even though the computational effort of evaluating the embedding energy is similar to that for the pairwise-additive interactions.

The functional form of the pairwise additive term $\phi_{ij}(r)$ is:

$$\begin{aligned} \phi(r_{ij}) &= [Z(r_i)Z(r_j) - Z(r_{cut})Z(r_{cut})]/r, & r<r_{cut} \\ &= 0 & r \geq r_{cut} \end{aligned} \tag{3}$$

where $Z_m(r)$ is the effective charge of atom m and r_{cut} is chosen to be large enough that the pair interactions are very small at that value. The effective charge of an atom is given the functional form as follows:

$$Z(r) = Z_o(1 + \beta r^v)\exp(-\alpha r) \tag{4}$$

The atomic densities are approximated by the single-determinant Hartree-Fock calculations of Clementi and Roetti.[13] For nickel, the atomic density is further approximated as the sum of electron densities from the 3d and 4s shells, weighted by the number of electrons in each shell. We used the FBD parameters for all the calculations reported here.

The total configurational energy of the substrate and the adlayer, within the EAM model, is given by

$$U = \sum_{i=1}^{N_a} F_i(\rho_i) + \sum_{j=1}^{N_s} F_j(\rho_j) + \sum_{\substack{i=1 \\ i'>i}}^{N_a} \varphi_{ii'}(r_{ii'}) + \sum_{\substack{j=1 \\ j'>j}}^{N_s} \varphi_{jj'}(r_{jj'}) + \sum_{i=1}^{N_a}\sum_{j=1}^{N_s} \varphi_{ij}(r_{ij}) \qquad (5)$$

where N_a and N_S are the number of adlayer and substrate atoms, $F(\rho)$ is the embedding energy of the metal atom under consideration, and $\varphi(r)$ is the short-range pairwise additive interaction terms. The electron densities ρ's are given by

$$\rho_i = \rho_i^a + \sum_{j=1}^{N_s} \rho_j(r_{ij}) \qquad (6)$$

where $\rho_i^a = \sum_{i' \neq i}^{N_a} \rho_{i'}(r_{ii'})$ is the electron density of the atoms in the isolated adlayer and ρ_i is the electron density in presence of the substrate.

$$\rho_j = \rho_j^s + \sum_{i=1}^{N_a} \rho_i(r_{ij}) \qquad (7)$$

where $\rho_j^s = \sum_{j' \neq j}^{N_s} \rho_{j'}(r_{jj'})$ is the electron density of the atoms in the isolated substrate and ρ_j is the electron density in presence of the adlayer.

The simple pairwise additive potential, adapted in the benchmark calculations, are given by

$$U(r) = 4\varepsilon \exp\left\{-\frac{8}{3}\left[\left(\frac{r}{\sigma}\right)^2 - 1\right]\right\}\left(\exp\left\{-\frac{8}{3}\left[\left(\frac{r}{\sigma}\right)^2 - 1\right]\right\} - 1\right) \qquad (8)$$

The parameter σ is fixed according to the scheme followed in earlier studies[7b] excepting that for considering the interactions between adatoms in one set of calculations, we have set $\varepsilon = 1$ for adatom-substrate and $\varepsilon = 1/3$ for adatom-adatom interactions.

III. RESULTS and DISCUSSION

Energetics of fcc (111) / fcc(100) Structure

The energy characteristics with and without the $U_{a\text{-}a}$ interactions as a function of the lattice-constants ratio, $P = a_a/a_s$, with fixed relative orientation $\theta = 0°$ are shown in fig.1 (panels a' and a respectively) using the pairwise additive potentials of equation (8). In the previous studies[7b], the details of the direction and the order of axial commensuration and of the partial commensuration are not only discussed at length but also have been identified in terms of the maxima and minima in the

energy seen in panel a. While there may exist a P which minimizes $U_{a\text{-}s}$, considering only the $U_{a\text{-}s}$ interactions does not minimize the real total energy of the system due to the effect of $U_{a\text{-}a}$. Considering both $U_{a\text{-}s}$ and $U_{a\text{-}a}$ leads to the disappearance of energy maxima (at lower values of P) corresponding to the lower order axial commensuration in the x-direction.

The total energy of the adlayer and substrate within the EAM scheme (adapting the EAM models for Cu and Ni) has converged at $Z = 0.60\ a_s$ which is comparable to $Z = 0.63\ a_s$ obtained with simple pairwise additive potential. The variation of energy with P, using the EAM model, are shown in the lower most panel of figure 1. Excepting for the deep minimum around P = 1.01 the remaining energy characteristics appear to be absent. In order to address this issue of lack of structure in the energy curves with EAM model and to examine the dependence of the energy characteristics on the interaction potential model, namely a simple pairwise additive versus realistic EAM model, we first examined the individual energy contributions from the embedding energy term and short range interactions to the total energy of the Cu (111)/Ni (100) structure.

Using equations (5)-(7), the embedding and the short-range contributions for the isolated adlayer and the adlayer as well as for the total structure consisting of both adlayer and substrate as a function of P has been evaluated and shown in figure 2. Upon interfacing the substrate with adlayer and vice-versa, the electron density increases which reduces in a more negative embedding energy compared to the isolated structure. This can be clearly seen by examining the $F(\rho)$ curves in figure 2. As the geometry of the substrate does not change in these energetics calculation (rigid substrate lattice), the embedding energy contributions for the isolated substrate has to be subtracted from the total energy values. The net $F(\rho)$ for the substrate interfacing with the adlayer is also shown in figure 2.

The short-range repulsive interactions between the adatom-adatom and adatom-substrate are also shown in figure 2. The adatom-adatom short-range energy contribution to the total energy (U in equation 5) has the expected behavior as a function of P, whereas the adatom-substrate short-range energy exhibits (not shown clearly in figure 2 but can be seen in the panel c of figure 3 described below) similar energy characteristics as that of panel a in figure 1. This led to the exploration of obtaining a reasonable estimate of the contribution from the embedding energy interaction in order to estimate the total energy of the adlayer-substrate interactions by adding it to the short-range repulsive interaction between adatom and substrate atoms. Within the EAM scheme, the absolute values of the embedding energy contribution to such an interfacial structure (mixed interaction) is not clearly defined, but the following phenomenological scheme has been adapted.

Using equations (9) and (10), the total interaction energy of the adatom-adatom structure and substrate-substrate structure as a function of P is obtained using separately a fixed electron

density appropriate to the substrate and to the adlayer corresponding to a reasonable interface geometry within the P space.

$$U_{a-a} = \sum_{i=1}^{N_a} F_i(\rho_i^a + \rho_i^{s_f}) + \sum_{\substack{i=1 \\ i'>i}}^{N_a} \varphi_{ii'}(r_{ii'}) \qquad (9)$$

where ρ^{s_f} is the electron density of the substrate at a fixed geometry of the interface (substrate and adlayer), i.e. at a fixed lattice mismatch as seen by each of the adlayer atoms .

$$U_{s-s} = \sum_{j=1}^{N_s} F_j(\rho_j^s + \rho_j^{a_f}) + \sum_{\substack{j=1 \\ j'>j}}^{N_s} \varphi_{jj'}(r_{jj'}) \qquad (10)$$

where ρ^{a_f} is the electron density of the adlayer at a fixed geometry of the interface (substrate and adlayer), i.e. at a fixed lattice mismatch which is felt by each of the substrate atoms.

The total energy of the adatom-substrate interaction is then obtained by taking the difference between the total energy (as given in equation 5) of the interface under consideration and that of the adatom-adatom and substrate-substrate atomic interactions from equations (9) and (10). This yields an expression for the adsorbate-substrate interaction

$$\begin{aligned} U_{a-s} &= U - U_{a-a} - U_{s-s} \\ &= \sum_{i=1}^{N_a} \left\{ F_i(\rho_i) - F_i(\rho_i^a + \rho_i^{s_f}) \right\} + \sum_{j=1}^{N_s} \left\{ F_j(\rho_j) - F_j(\rho_j^s + \rho_j^{a_f}) \right\} \\ &\quad + \sum_{i=1}^{N_a} \sum_{j=1}^{N_s} \varphi_{ij}(r_{ij}) \end{aligned} \qquad (11)$$

For a series of fixed geometries of the interface, the above scheme has been adapted in order to assess the accuracy in choosing the fixed geometries of the interface and the results for the fixed geometries corresponding to P = 0.8 and 1.4 has been reported in figure 3. Panels a and b show the total $F(\rho)$ (continuous line curve) contribution (sum of the first two terms in equation 11) to the total adatom-substrate interaction energy as well as the the individual energy terms due to the adlayer (first term in equation 11, short-dashed curve), of the substrate (second term in equation 12, long-dashed curve). The adatom-substrate short-range energy contribution

(continuous line curve) as shown in panel c exhibits energy characteristics similar to the simple model results shown in figure 1, panel a. Comparison of the continuous lines in the three panels in figure 3 indicate that the embedding and short-range repulsive energies balance out in terms of their characteristics, i.e., maxima in one is a minima in the other, and the magnitude of $F(\rho)$, although depends on the chosen fixed geometry, is much less than that of short-range repulsive energy. Thus the energy characteristics of the total adatom-substrate interaction energy (short-dashed and long-dashed curves corresponding to the two fixed geometries) are same as that of those obtained from simple pairwise additive potentials. This has two implications: the primary implication is that the recent careful examination[7b] of the conditions in terms of axial commensuration necessary to obtain a coherent interface between various such dissimilar structures, based on detailed studies with simple pairwise additive potentials, can be used as a pointer. The second implication appear to confirm another previous simple model dependent study[7a] which has shown that the energy characteristics are independent of the long-range attractive part of the potential indicating that for rigid lattices the energetics are only determined by the relative atomic sizes of the substrate and monolayer.

Strain at Cu(100)/Ni(100) and Ni(100)/Cu(100) Interfaces

The strain at the interface can be defined as Strain (%) = $(b - a_a)/a_a$, where b is the strained lattice constant (varying lattice constant in the calculation) and a_a is the unstrained (corresponding to the bulk value) lattice constant of the adsorbate. The total energy of the interface was calculated as a function of the strain (varying adalyer lattice constant). The energy curve shows a minimum with respect to strain, which is dependent on the number of atoms in the adlayer. The energy vs strain for three different sizes of the adlayer are shown in figure 4. The energy difference at the zero strain and the energy at the minimum of the strain is taken to be the strain energy. In our calculations on Ni/Cu and Cu/Ni the minimum energy was at strain (%) ~ ± 2.5 - ± 2.6. The strain energy as a function of number of adatoms increases monotonically until N = 121 and a sharp increase in strain energy occurs. This might indicate that clusters with 81 or more atoms will have such a strain, the origin of which is not clear. The question of how large must a cluster be before dislocations form must be investigated

Recent studies[7b] have shown that the strain energy as a function of the square root of the total number of adsorbate atoms becomes constant at some value of N, which is called N(crit) implying that the adsorbate cluster becomes stable to the addition of more adatoms. These studies indicate the prediction of a large uniform monolayer coverage. A more useful and pertinent quantity is probably the critical size of atoms above which the monolayer is no longer stable on the surface and tends to force dislocations rather than continue the monolayer growth. Comparison of

the energetics of these two situations (large monolayer vs several small clusters on the surface) would give a nice indication of what the system wants to do.

The strains and the energies at the interfaces of Cu/Ni(100) and Ni/Cu(100) corresponding to the positive and negative misfit respectively are shown in figure 5. The strain energy for the positive misfit interface (Cu/Ni) is larger than that of the negative misfit interface (Ni/Cu, see fig.5). Based on the continuum limit for the strain energy in terms of the generalized elastic constant, Y, the thickness (t) of the overgrowth, and the strain (e), $E_{strain} = Y\,t\,e^2$, the large value of Y for the positive misfit would give a substantially reduced value of t_c, the critical thickness beyond which pseudomorphism is not possible. Furthermore, a large number of layers are expected to grow for a smaller strain energy per monolayer. Thus it implies that a large number of layers will grow pseudomorphically in the case of negative misfit interface. This type of estimate is of great interest in the fabrication of superlattices made up of lattice mismatched materials.

IV. SUMMARY AND CONCLUSION

The similarity of the results obtained from these studies using realistic interaction potential model for the metallic structures and from the previous detailed studies based on model potentials suggest that for rigid lattices the energetics are determined by the relative atomic sizes of the substrate and monolayer. The strain energy for the positive misfit interface (Cu/Ni) is larger than that of the negative misfit interface (Ni/Cu). This indicates that a large number of layers will grow pseudomorphically in the case of negative misfit interface. This type of estimate is of great interest in the fabrication of superlattices made up of lattice mismatched materials. The diffusion and the strain energy dependence on the substrate orientation may provide a clue to the choice of substrate orientation for obtaining better quality films.

ACKNOWLEDGEMENT

This work was supported by the Air Force Officers Scientific Research under grant number F49620-88-C-0086. It is a pleasure to acknowledge useful discussions with Dr. Bruce Garrett regarding the separation of reasonably realistic contribution from the embedding energy to the total adatom-substrate interaction energy. We acknowledge San Diego Supercomputer Center for a reasonable support of supercomputer time at their facility.

REFERENCES

1 Ch. 2, 5, 8, and 9, in Epitaxial Growth , ed. by J. W. Mathews (Academic, N. Y., 1975)

2 Ch. 1, 5, and 6, in Synthetic Modulated Structures ed. by L. C. Chang and B. C. Giessen (Academic, N. Y., 1985).

3 I. K. Schuller and C. M. Falco, in VLSI Electronics: Microstructure Science, ed. by N. G. Einpruch, Vol. 4, p. 183 (Academic, N Y., 1982); ref. 2, Ch. 10.

4 F. C. Frank and J. H. van der Merwe, Proc. R. Soc. London, **A198**, 205, 216 (1949); ibid, **A200**, 125 (1949).

5 L. A. Bruce and H. Jaeger, Phil. Mag. **A38**, 223 (1978)

6 J. H. van der Merwe, Phil. Mag. **A45**, 145, 159 (1982).

7 (a) R. Ramirez, A. Rahman, and I. K. Schuller, Phys. Rev. **B30**, 6208 (1984); (b) A. Kobayashi and S. Das Sarma, Phys. Rev. **B35**, 8042 (1987)

8 (a) M. S. Daw and M.I. Baskes, Phys. Rev. **B29**, 6443 (1984); (b) A. F. Voter and S. P. Chen, MRS proceedings, Winter 1986, Symposium I; (c) M. W. Finnis and J. E. Sinclair, Phil. Mag. **A50**, 45 (1984); (d) K. W. Jacobsen, J. K. Norskov, and M. J. Puska, Phys. Rev. **B35**, 7423 (1987).

9 (a) F. H. Stillinger and T. A. Weber, Phys. Rev. **B31**, 5262 (1985); (b) K. Ding and H. C. Andersen, Phys. Rev. **B34**, 6987 (1986); (c) R. Biswas and D. R. Hamann, Phys. Rev. Lett. **55**, 2001 (1985) and Phys. Rev. **B36**, 6434 (1987); (d) J. Tersoff, Phys. Rev. Lett. **56**, 632 (1986); (e) B. W. Dodson, Phys. Rev. **B33**, 7361 (1986); ibid. **35**, 2795 (1987); (i) M. I. Baskes Phys. Rev. Lett. 59, 2666 (1987).

10 (a) V. L. Moruzzi, P. M. Marcus, K. Schwarz, and P. Mohn, Phys. Rev. **B34**, 1784 (1986); (b) P. M. Marcus, V. L. Moruzzi, Z. Q. Wang, Y. S. Li, and F. Jona, in Physical and Chemical Properties of Thin Metal Overlayers and Alloy Surfaces, MRS Symposia Proceedings, Vol. 83, ed. D. M. Zehner and D. W. Goodman (MRS, Pittsburgh, PA, 1987); (c) R. E. Watson, M. Weinert, and J. W. Davenport, Phys. Rev. **B35**, 9284 (1987); (d) G. P. Srivastava and D. Weaire, Adv. Phys. **36**, 463 (1987) and references therein.

11 C. S. Murthy, B. M. Rice, and M. J. Redmon, "Growth Studies of Metal-Metal/Semiconductor Structures", AFOSR SBIR Phase I Report (1989).

12 S. M. Foiles, M. I. Baskes and M. S. Daw, Phys. Rev. **B 33**, 7983 (1986).

13 E. Clementi and C. Roetti, Atomic and Nuclear Data Tables (Academic, New York, 1974), Vol. 14, Nos. 3 and 4.

Figure Captions

Figure 1. Energy per adsorbate atom vs lattice constant ratio, a_a/a_s, for the interfacial structure, fcc (111) / fcc (100) with a fixed relative orientation of $\theta = 0°$. Panels (a) and (a') refer to the results obtained from using a traditional central potential. The panel a' and the energies from the EAM model for Cu (111)/Ni(100) includes the adatom-adatom interactions.

Figure 2. The embedding energy, $F(\rho)$, per adsorbate atom vs lattice constant ratio, a_a/a_s, for the isolated Ni adlayer (continuous line curve) and the Ni adlayer (dashed line curve) on the Cu substrate and the variation of short-range pairwise interaction energy, and $\varphi(r)$, per adsorbate atom (RHS ordinate scale) of the adlayer with a_a/a_s. The flat dot-dashed curves refer to the change in $F(\rho)$ for the substrate interfaced with adlayer and $\varphi(r)$ for the adatom-substrate interactions.

Figure 3. Variation of the individual energy, $F(\rho)$ and $\varphi(r)$, contributions and the total configurational energy, U (r) per adsorbate atom with a_a/a_s for the adlayer-substrate interactions. Panels a and b refer to $\rho^{a}{}_{f}$ and $\rho^{s}{}_{f}$ for fixed geometries (see text) of the interface a_a/a_s corresponding to $a_a/a_s = 0.8$ and 1.4 respectively: short-dashed curve is for the adlayer, long-dashed curve is the substrate embedding energy contributions and continuous curve is the total embedding energy, $F(\rho)$, part in the adlayer-substrate interaction energy. In Panel c, the continuous curve represents the short-range pairwise interaction energy, $\varphi(r)$, for the adatom-substrate interactions, and short- and long-dashed curves correspond to the the sum of $\varphi(r)$ and $F(\rho)$ for the two fixed geometries considered respectively.

Figure 4 The total configurational energy of the Cu (100)/Ni (100) interface as a function of strain and as a function of the number of adsorbate atoms (25, 49, and 81). The energies corresponding to zero strain and the minimum is marked with symbols.

Figure 5 The total configurational energy of the Cu (100)/Ni (100) and Ni (100)/Cu (100) interfaces as a function of strain. The abscissa and ordinate scales for the Ni/Cu structure are on the top and RHS.

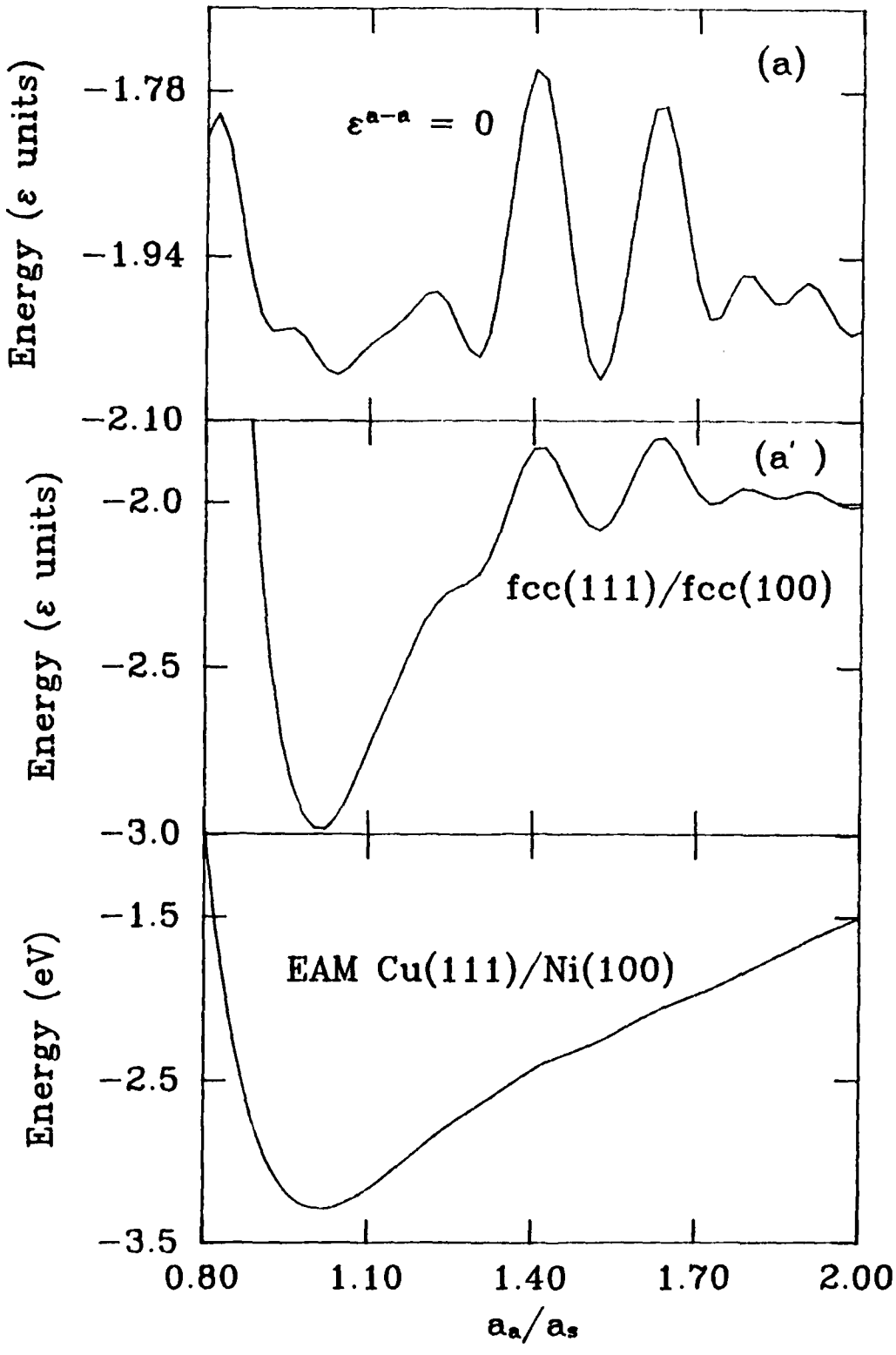
(a)
$\varepsilon^{a-a} = 0$
−1.78
−1.94
−2.10
Energy (ε units)
(a')
fcc(111)/fcc(100)
−2.0
−2.5
−3.0
Energy (ε units)
EAM Cu(111)/Ni(100)
−1.5
−2.5
−3.5
Energy (eV)
0.80
1.10
1.40
1.70
2.00
a_a/a_s

FIG. 1

Interfacial Energy Contributions: EAM Cu/Ni

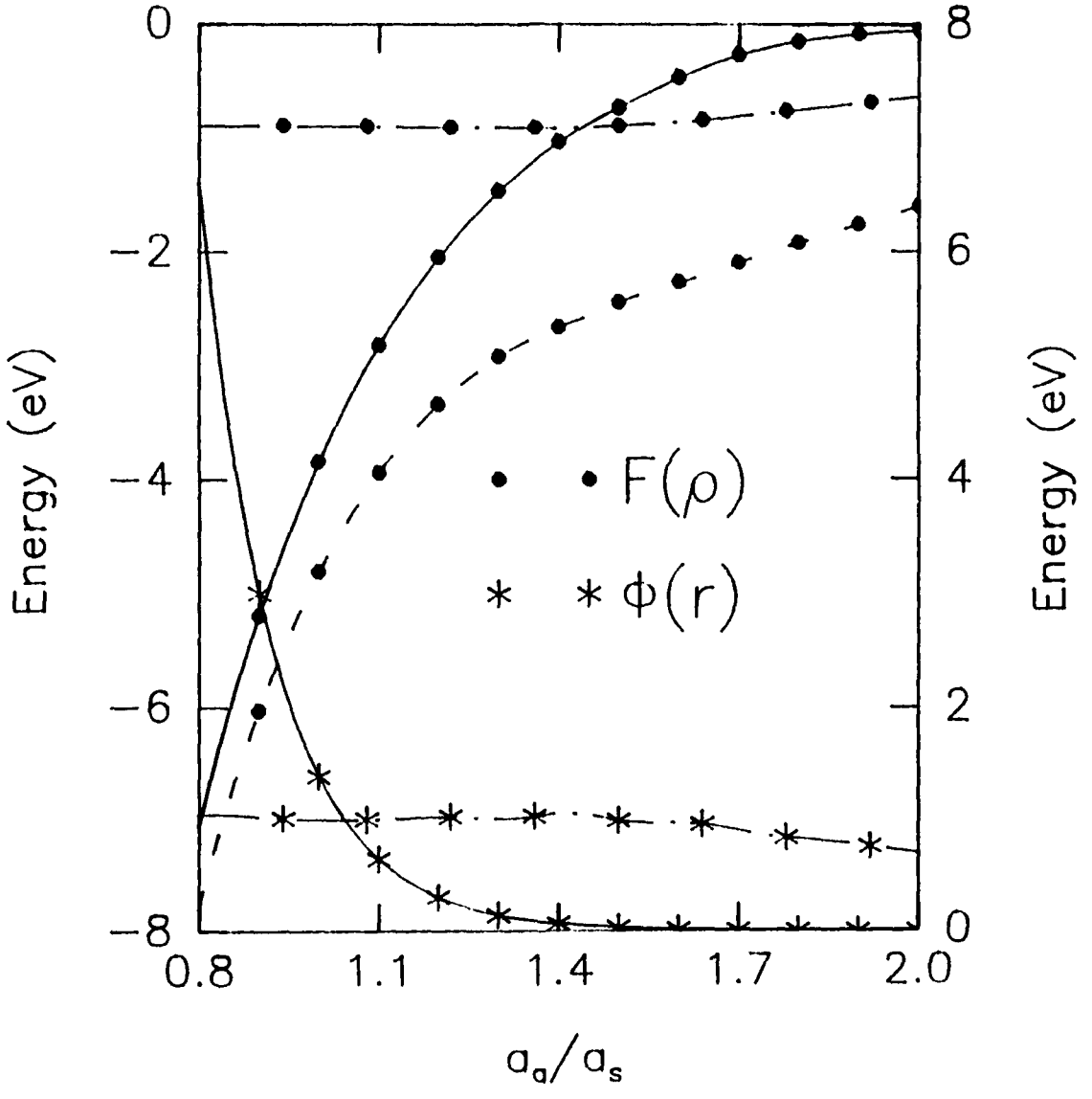

FIG. 2

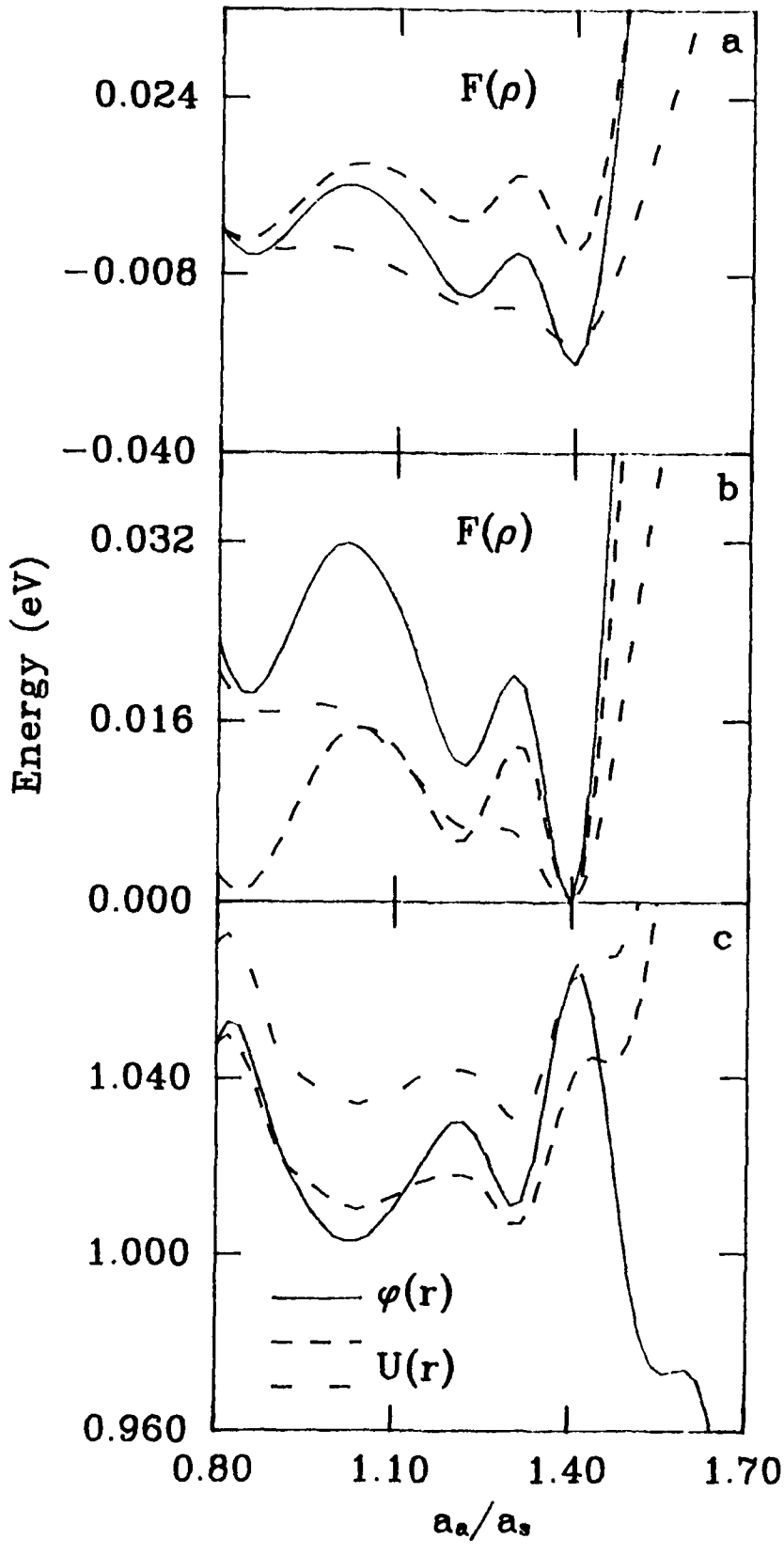
a
F(ρ)
0.024
−0.008
−0.040
b
F(ρ)
0.032
0.016
0.000
c
1.040
1.000
0.960
φ(r)
U(r)
Energy (eV)
0.80
1.10
1.40
1.70
a_a/a_s

FIG. 3

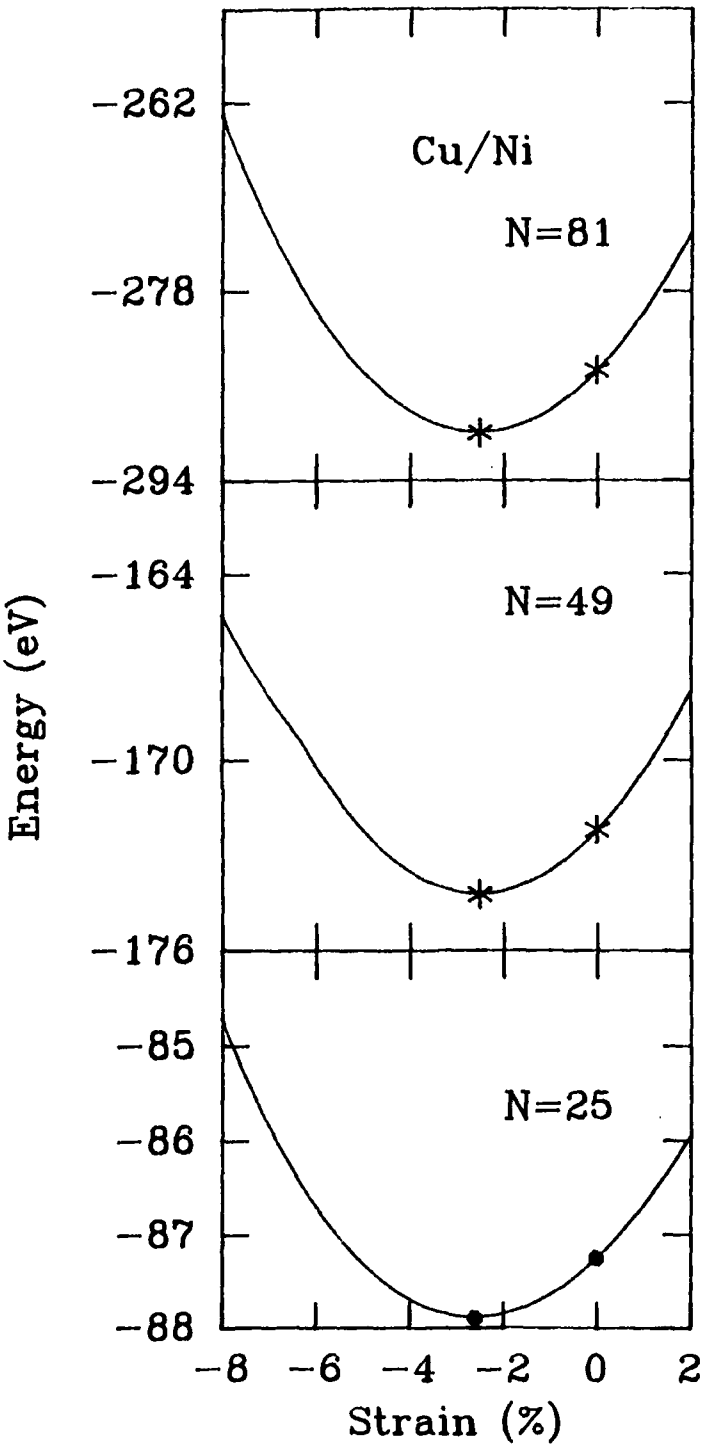
Cu/Ni
N=81
N=49
N=25
−262
−278
−294
−164
−170
−176
−85
−86
−87
−88
Energy (eV)
−8
−6
−4
−2
0
2
Strain (%)

FIG. 4

Strain at Positive and Negative Misfit

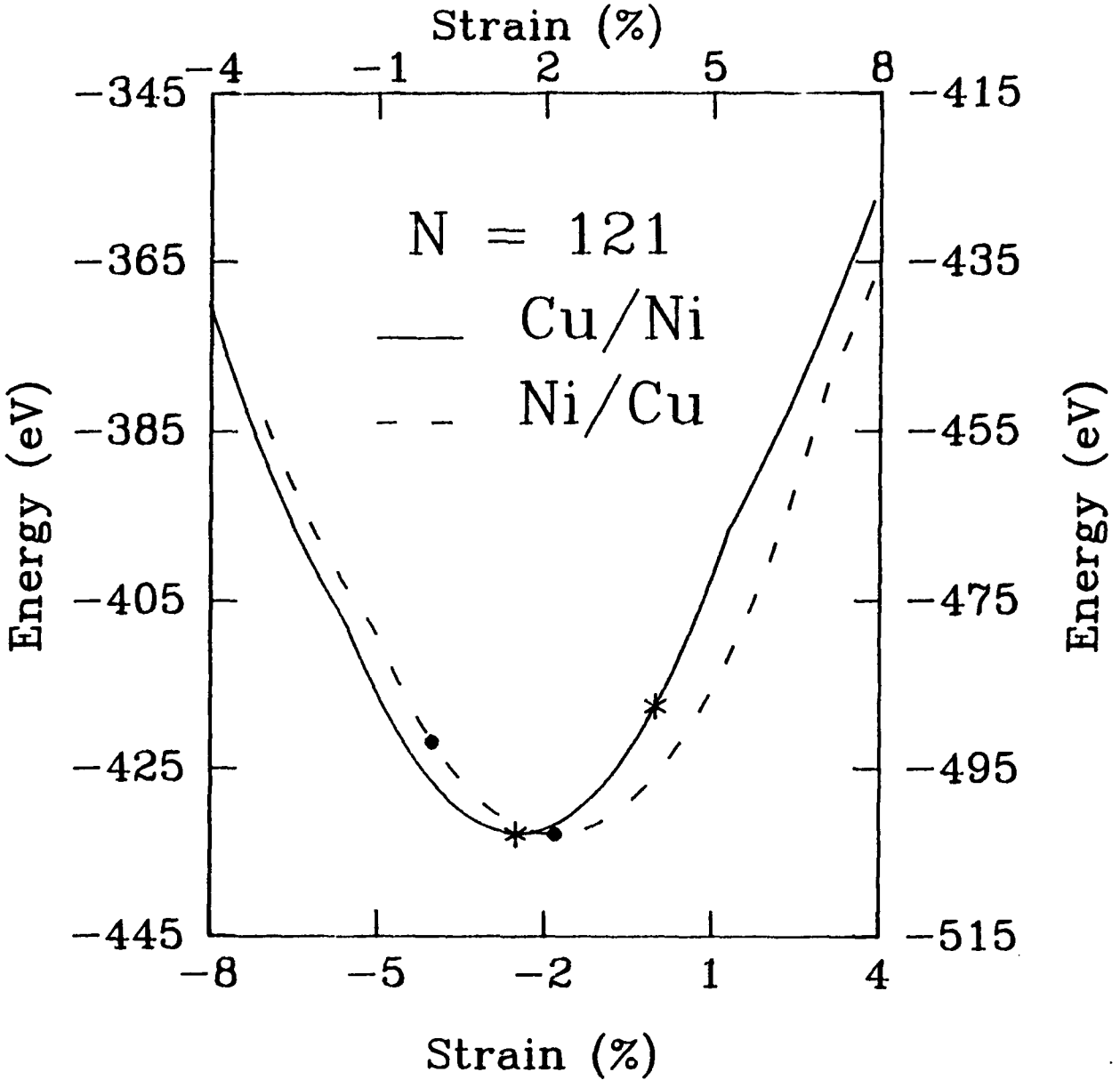

FIG. 5

APPENDIX-2

Comparative Study of Embedded-Atom Method Potentials: Self-Diffusion on FCC Metallic Surfaces

Preliminary Version

Comparative Study of Embedded-Atom Method Potentials: Self-Diffusion on FCC Metallic Surfaces

B. M. Rice, C. S. Murthy, M. J. Redmon, and B. C. Garrett
Chemical Dynamics Corporation*
Upper Marlboro, MD 20772

* Mailing Address: 9560 Pennsylvania Avenue, Suite 106, Upper Marlboro, MD 20772

Abstract

Several potential models [S. M. Foiles, M. I. Baskes, and M. S. Daw, Phys. Rev. B 33, 7983 (1986); A. F. Voter and S. P. Chen, Mater. Res. Soc. Symp.82, 175 (1987); D. J. Oh and R. A. Johnson, J. Mater. Res. 3, 471 (1988) and " Embedded Atom Method for Close-Packed Metals "Atomistic Modelling of Materials: Beyond Pair Potentials" ed. V. Vitek and D. J. Srolovitz , (Plenum to be published) World Materials Congress Proc. 1988; G. J. Ackland, G. Tichy, V. Vitek, and M. W. Finnis, Phil. Mag. 56, 735 (1987)] based on embedded-atom-method (EAM) have been adopted to study self-diffusion on Ni(100), -(111) and -(110) surfaces. The models consist of an effective pairwise additive (attractive electrostatic or purely repulsive) and a many-body cohesive (correspondingly repulsive or attractive) interactions parameterized to account for a majority of bulk and a few defect properties. Variational transition state theory calculations using these potentials provide Arrhenius parameters and diffusion coefficients, as well as a comparison among the four EAM potentials employed. Additionally, the results of these calculations are useful in assessing the currently parameterized EAM potentials for surface and interfacial dynamical studies. Discussion of the results is given in the light of available experimental data.

I. INTRODUCTION

Most processes occurring on a crystal surface and at interfaces are expected to be influenced by the kinetics of the atoms. The mobility of atoms on a crystal surface can indeed be orders of magnitude larger than in the bulk at the same temperature and become the determining step in many processes such as surface reconstruction, the rate of chemical reaction, and epitaxial growth. Diffusion on metals has received both experimental and theoretical attention.[1] Still, little is known about the microscopic mechanisms with which atoms move on a crystal surface. For instance, neither the role of the presence of steps or kinks, nor the chemical specificity is known. The relation between the surface diffusivity and surface structure has recently been undertaken by detailed molecular dynamics simulations using simple model potentials. These studies[2] have shown that the surface structure and the softness of the repulsive potential play a dominant role in determining the diffusion properties and that complicated migration mechanisms, such as exchange mechanism for adatom migration on channelled surface, are active for the migration of adatoms. The major goal of this study is to critically examine the use of embedded-atom-method (EAM)[3] potentials, which have been fitted to bulk metal properties, in dynamics calculations of surface and interfacial processes. We present results of dynamical calculations of diffusion of atomic nickel on several nickel surfaces using various EAM potentials.

Variational transition state theory (VTST)[4] has been used successfully in calculating rates of gas phase reactions. Additionally, it has been applied to other gas-surface diffusion studies.[5] However, as is the case with all theoretical dynamical studies, the calculation is accurate only to the degree that the potential energy surface correctly describes the system under study. While obtaining accurate first-principles potential-energy surfaces for small polyatomics is feasible, the same cannot be said for metallic materials because of the magnitude of the calculations. Therefore, the potential-energy surfaces used in calculations of metallic bonding interactions usually are global functions fit to reproduce experimentally measured data such as elastic modulii, equation of state, defect energetics, and diffusion rates, etc. Because an empirical approach must be taken in determining the potential-energy surfaces to use in interfacial growth related simulations at the atomistic level, it is desirable to have a physically motivated model. The EAM was developed within such a framework. Prior to development of EAM potentials, the most prevalent form of a potential for describing a solid involved pairwise terms only, fit to structural and thermodynamic data of the bulk metal.[6] However, this type of potential is inadequate due to the many-body nature of electron-core interactions inherent in a metallic material. Daw and Baskes, and Finnis and Sinclair have independently developed[3] a function which describes the potential-energy of a metallic solid in terms of the "embedding energy" of each atom in the crystal. This energy is a function of local electron density that the atom senses due to nearby atoms.

In this study of adatom diffusion, we will be using an EAM potential which is empirically adjusted to static bulk properties. In addition to examining the details of dynamics of the system, this calculation provides an opportunity to critically evaluate and refine the EAM potential, as well as indicating which properties of the system, pertinent to the dynamics of the interface, must be incorporated in the fit to correctly describe the system. The remainder of the paper is organized as follows. Section 2 provides the background and description of the EAM potentials used in this study and Section 3 briefly reviews the dynamical methods and describes the computational procedures. The structural models of the Ni lattices used in the calculations are described in Section 4, and the results of surface self-diffusion are presented in Section 5. Concluding remarks are given in Section 6.

II. POTENTIAL ENERGY SURFACES

The embedded atom method (EAM) was developed as a means of calculating realistic ground-state properties of metallic systems. The EAM is based on density functional theory and its derivation is given elsewhere.[3] Previous applications of the EAM to metallic systems have given good results. For example, energies and geometries,[3,7] structure of liquid metals,[8] bulk and surface phonons,[9] surface relaxations, reconstructions and other surface phases of transition metals,[10] point defect properties and basic alloy properties[3a] calculated with EAM are in good agreement with experiment. Additionally, applications to hydrogen-metallic systems have successfully predicted ordered structures, critical temperatures, and the influence of hydrogen on dislocation motion and fractures.[3b,11] Its success in predicting a wide variety of phenomena in metallic systems, coupled with its low computational demands, makes it a highly desirable alternative to the commonly used and often inadequate pairwise potentials in describing metallic systems.

In the embedded atom method the energy of a collection of atoms is expressed as a sum of a density-dependent embedding energy and a pair interaction term:

$$U = \sum_i F_i(\rho_i) + \frac{1}{2}\sum_{i \neq j} \phi_{ij}(r_{ij}) \qquad (1)$$

where $F_i(\rho_i)$ is the energy needed to embed atom i into the local electron density, ρ_i, of the surrounding atoms, and ϕ_{ij} is a pair potential between atoms i and j. Different schemes have been used to describe the local electron density and the pair interactions of Eq. (1) for Ni; they are summarized below.

In the Foiles, Baskes and Daw (FBD) approach, the local electron density ρ_i into which atom i is embedded is approximated by the sum over atomic electron densities $\rho_j^a(r_{ij})$ from all other atoms in the system:

$$\rho_i = \sum_{i \neq j} \rho_j^a(r_{ij}) \tag{2}$$

This functional form has the advantage of including many-body interactions due to the non-linear nature of the embedding function even though the computational effort of evaluating the embedding energy is similar to that for the pairwise-additive interactions.

The functional form of the pairwise additive term $\phi_{ij}(r)$ is:

$$\begin{aligned} \phi(r_{ij}) &= [Z(r_i)Z(r_j) - Z(r_{cut})Z(r_{cut})]/r, & r<r_{cut} \\ &= 0 & r \geq r_{cut} \end{aligned} \tag{3}$$

where $Z_m(r)$ is the effective charge of atom m and r_{cut} is chosen to be large enough that the pair interactions are very small at that value. The effective charge of an atom is given the functional form as follows:

$$Z(r) = Z_o(1 + \beta r^v)\exp(-\alpha r) \tag{4}$$

The atomic densities are approximated by the single-determinant Hartree-Fock calculations of Clementi and Roetti.[12] For nickel, the atomic density is further approximated as the sum of electron densities from the 3d and 4s shells, weighted by the number of electrons in each shell. The number of 4s electrons, N_s, is used as an adjustable parameter and is set to 2 for all the calculations reported here.

The parameters are fitted to experimental data (equation of state, elastic modulii, defect energetics, data pertaining to the transition metallic alloys) by a least squares procedure and those defining the pair interactions for nickel are given.[3a] In the fitting procedure, all of the parameters for the Ni-Ni interactions are first fitted[13] to the bulk lattice constant, sublimation energy, elastic constants and vacancy formation energy with the exception of the value of N_s. For a given set of parameters for the atomic densities and pair interaction terms, the embedding function for nickel is adjusted so that the simplified equation of state of the metal.[14] is exactly reproduced for successive values of the density. Thus the embedding function for Ni is represented numerically, and in the present application is fitted to a cubic spline

The differences between the FBD[7] and other approaches are primarily found in the derivation and interpretation of the embedding density of the electron surrounding the atom, ρ, and the embedding function $F(\rho)$. Voter and Chen (VC)[15] have basically followed the FBD[7] scheme excepting for adopting a functional form for the embedding energy (instead of the numerical scheme of FBD) and a Morse-type function for the short-range interaction. Furthermore, in contrast to FBD, VC have modelled the embedding term as a repulsive interaction.

Oh and Johnson's[16] approach was to develop an EAM model with simple functional forms which result in fewer parameters to fit and thus provide easy access to the EAM model on any type of the computer. While Ackland, Tichy, Vitek, and M. W. Finnis (ATVF),[17] following Finnis and Sinclair,[3b] used a square-root function for $F(\rho)$ and identified $F(\rho)$ with the second moment of the density of states and their functional forms both for $F(\rho)$ and $\phi(r)$ consist of a series expansion with built in step-functions, the coefficients of which have been fitted to the experimental data as well as the pressure-volume data from first-principles calculations.

III. COMPUTATIONAL METHODS

For diffusion on a surface, in which all binding sites are equivalent, the diffusion coefficient can be related to the hopping rate between adjacent sites provided the following assumptions are true:

(1) The concentration of adsorbate atoms is sufficiently low so that the adsorbate atoms do not interact with one another;

(2) Diffusion occurs through a series of uncorrelated hops from one binding site to another adjacent one; and

(3) The hopping from one binding site to another can be treated as an individual unimolecular process with thermal rate constant k(T).

This random walk model of diffusion gives a relation between the thermal diffusion coefficient D(T) and the unimolecular rate constant, k(T), as follows:[18]

$$D(T) = \frac{a^2}{2\gamma} k(T) \tag{5}$$

where a is the hop length, and γ is the dimensionality of the system (γ=2 for diffusion on a surface wherein all binding sites are equivalent, γ=1 for surface diffusion along channels (such as diffusion along the [110] direction on Ni(110) or along the [001] direction on Ni(110)).

The rate constant k(T) is calculated from canonical VTST with semiclassical adiabatic ground state transmission coefficients. The computational procedures used here are similar to those used for gas-phase reactions,[4] and details of the modifications needed to treat diffusion on surfaces are outlined elsewhere.[5] In review, the procedure consists of first locating the reactant, product and saddle point geometries (locations at which the gradient vanishes) then determining the reaction path by following the negative of the gradient vector in mass weighted coordinates from the saddle point down into the reactant and product geometries. The reaction coordinate s is defined as the distance along the reaction path from the saddle point and, by convention, is negative on the reactant side of the saddle point. The generalized transition state theory rate is expressed in terms of the location of transition state along the reaction coordinate

$$k^{GT}(T, s) = \sigma \frac{k_B T}{h} \frac{Q^{GT}(T, s)}{Q^{R}(T)} \exp\left(-V_{MEP}(s)/k_B T\right) \tag{6}$$

where $Q^{GT}(T,s)$ is the partition function for the bound degree of freedom at the generalized transition state location at s, and $V_{MEP}(s)$ is the potential along the reaction path. In canonical variational transition state theory (CVT) the location of s is optimized to minimize the rate.

The generalized transition state partition functions are evaluated quantum mechanically using the independent normal mode approximation which neglects all anharmonic coupling between the modes. The energy levels for the individual modes are computed harmonically unless otherwise noted.

Quantum mechanical effects on the bound vibrational motion are included by treating the partition functions quantally, and quantal effects on reaction coordinate motion are treated using multiplicative semiclassical ground-state adiabatic transmission coefficients

$$k^{CVT/G}(T) = \kappa^{G}(T)\, k^{CVT}(T) \tag{7}$$

Within the adiabatic approximation, the effective barrier along the reaction path is obtained from

$$V_a^G(s) = V_{MEP}(s) + \varepsilon^{GT}(s, \alpha = 0) \tag{8}$$

where $\varepsilon^{GT}(s,\alpha=0)$ is the ground-state energy level for the bound vibrational modes at the generalized transition state located at s. The transmission coefficients are obtained from Boltzmann averages of the probabilities for tunneling through the ground-state adiabatic barrier

$$\kappa^{G}(T) = \frac{\exp\left(V^{A}/k_B T\right)}{k_B T} \int_0^\infty dE\; P^{G}(E)\, e^{-E/k_B T} \tag{9}$$

where V^A is the value of the ground-state barrier at its maximum and E is the total energy. For the unimolecular process considered here the reactant and product species correspond to local wells in the adiabatic potential separated by the adiabatic barrier. For this case, eq. (9) is only an approximation since tunneling does not occur for a continuum of translational energies but from discreet energy levels in the bound wells of the adiabatic potential

$$\kappa^{GD}(T) = \exp\left(V^{A}/k_B T\right) \sum_{v} P^{G}(E_v)\, \exp\left(-E_v/k_B T\right) \tag{10}$$

In the limit of a large number of bound energy levels in the adiabatic potential eqs. (9) and (10) will be equivalent. However, for the systems studied, tunneling was not important.

IV. LATTICE MODELS

The structural model used in Ni diffusion on Ni(100) consists of 162 Ni atoms over four layers; 41 atoms are in each of the 1st and 3rd layers, and 40 atoms are in each of the 2nd and 4th layers. The eight atoms surrounding the reactant and product sites were allowed to move. These

were the six surface atoms surrounding the reactant and product sites and the two 2nd-layer atoms lying directly beneath the reactant and product sites.

The model of the Ni(111) crystal consists of 120 nickel atoms with four layers. There are 27 atoms in the first and fourth layers, and 33 atoms are in the second and third layers. The four surface atoms and three second-layer atoms adjacent to the reactant and product sites were allowed to relax.

Two different models were used in the Ni(110) calculation, because there are two different diffusional directions; one along the $[1\bar{1}0]$ direction and the other along the [001] direction. The model for calculation of nickel diffusion in the $[1\bar{1}0]$ direction consists of 186 atoms over five layers. There are 42 atoms in the first, third and fifth layers, and 30 atoms in the second and fourth layers. In this model, seven atoms were allowed to relax; the four surface atoms and the three second-layer Ni atoms adjacent to the reactant and product sites. The model for calculation of nickel diffusion in the [001] direction has 219 atoms, with 49 atoms in each of first, third and fifth layers and 36 atoms in each of the second and fourth layers. Atoms (six in first layer and four in the second layer) adjacent to reactant and product sites were allowed to move. The number of atoms allowed to move in any of the crystal model studied was not varied to check for convergence of a diffusion rate. The substrate model was arbitrarily chosen and used in each calculation for comparative purposes.

V. RESULTS

Nickel binds in a four-fold site above the Ni(100) surface plane, directly over a second-layer nickel atom. Rates of nickel diffusion from one four-fold binding site on a Ni(100) surface to an adjacent one were calculated using eq. 5 and a hop length of 2.4890 Å for the four EAM potentials. Comparison of the calculated diffusion coefficients obtained using the various EAM models as well as the available experimental data[19] is shown in Figure 1. Additionally, the calculated Arrhenius parameters for the four EAM potentials are listed in Table I.

Nickel can diffuse along two different channels on the (110) surface; the $[1\bar{1}0]$ and [001] directions. The calculated diffusion coefficients are shown in Figures 1 and 2 for the $[1\bar{1}0]$ and in figure 2 [001] diffusion together with the available experimental data.[20] Figure 2 exhibits experimentally observed directional anisotropy on 110 surfaces. The available experimental data at low temperatures refer to the intrinsic surface diffusion which is expected to be lower than that of intrinsic surface diffusion. The Arrhenius parameters for the (110) surface are also litsed in Table I, and the geometries and energetics, reported in Table II, clearly show that diffusion will occur much more readily along the $[1\bar{1}0]$ direction than along the [001] direction, due to the lower diffusional barrier along this channel.

Rates of Ni diffusion on Ni(111) were not calculated because of low barriers to diffusion. As shown in Table II, the classical diffusion barrier is less than 0.09 eV for all EAM potentials. When the barriers are too low, the approximation of uncorrelated hops becomes invalid, and other approaches for calculating diffusion coefficients are needed.

VI. SUMMARY AND CONCLUSION

Calculations of Nickel surface self-diffusion based upon variational transition state theory were performed using different types of embedded atom method potentials in an effort to to analyze the suitability of the currently parameterized potentials in calculating surface and interfacial properties. Stringent comparison with experiment is difficult due to (a) the lack of a quantitative relationship between the intrinsic (corresponding to an ideal flat surface) and mass transfer (involving the complex processes of the formation of surface defects and their migration) surface diffusion data as a function of temperature, the former being consistent with the calculations, and (b) the existence of contradictory data for the difference in the measured intrinsic and mass transfer data as well as large scatter in the experimental data. All the models exhibit the directional anisotropy for the self diffusion on Ni (110) surface. At high temperatures, the models agree with each other but as temperature decreases the predicted diffusion data fall within a scatterband.

Comparison of the classical diffusion barrier for Ni/Ni (100), Ni/Ni (110), and Ni/Ni(111) indicates that diffusion will occur more readily on (111) surface orientation. This may imply that the homoepitaxial growth will be relatively complete for (111) substrate orientation. These studies involving the surface diffusivity and surface structure with realistic interaction potentials as well as the explosive developments in the growth techniques should result in renewed impetus for accurate measurements of adatom diffusion.

ACKNOWLEDGEMENT

This work was supported by the Air Force Officers Scientific Research under grant number F49620-88-C-0086. We acknowledge San Diego Supercomputer Center for a reasonable support of supercomputer time at their facility.

REFERENCES

1 (a) Ehrlich and K. Stolt, Ann. Rev. Phys. Chem. **31**, 603 (1980); (b) J. D. Doll and A. F. Voter, Ann. Rev. Phys. Chem. **38**, 413 (1987); (c) H. P. Bonzel, in "Surface Mobilities on Solid Materials, Fundamental Concepts and Applications" ed. Vu Thien Binh, p 230.

2 G.D. Lorenzi in "Computer Simulation in Physical Metallurgy" , ed. G. Jacucci, (D. Reidel Publishing Co. 1986). p.43.

3 (a) M. S. Daw and M. I. Baskes, Phys. Rev. Lett **50**, 1285 (1983); M. S. Daw and M. I. Baskes, Phys. Rev. B **29**, 6443 (1984); (b) M. W. Finnis and J. E. Sinclair, Phil. Mag. A **50**, 45 (1984).

4 D. G. Truhlar, A. D. Isaacson, and B. C. Garrett, in "Theory of Chemical reaction Dynamics", Vol. IV (CRC Press, Boca Raton, FL, 1983), p. 65.

5 (a) J. G. Lauderdale and D. G. Truhlar, Surf. Sci. **164**, 558 (1985); J. Am. Chem. Soc. **107**, 4590 (1985); J. Chem. Phys. **84**, 1843 (1985).(b) T. N. Truong and D. G. Truhlar, J. Phys. Chem. **91**, 6229 (1987); (c) T. N. Truong and D. G. Truhlar, J. Chem. Phys. **88**, 6611 (1988).

6 (a) See an excellent recent review by R. A. Johnson, in "Computer Simulation in Materials Science" ed. R. J. Arsenault, J. Beeler, and D. M. Esterling (ASM 1988); (b) See various papers in Interatomic Potentials and Crystalline Defects, ed. J. K. Lee (Metallurgical Society of AIME, New York 1981).

7 S. M. Foiles, M. I. Baskes and M. S. Daw, Phys. Rev. **B 33**, 7983 (1986).

8 S. M. Foiles, Phys. Rev. **B 32**, 3409 (1985).

9 M. S. Daw and R. L. Hatcher, Solid State Commun. **56**, 697 (1985).

10 (a) M. S. Daw, Surf. Sci. Lett. **166**, L161 (1986); (b) S. M. Foiles, Surf. Sci. **191**, 329 (1987); (c) M. S. Daw and S. M. Foiles, Phys. Rev. Lett . **59**, 2756 (1987); (d) S. M. Foiles, Surf. Sci. Lett. **191**, L779 (1987).

11 (a) M. S. Daw and S. M. Foiles, Phys. Rev. **B 35**, 2128 (1987); (b) S. M. Foiles and M. S. Daw, J. Vac. Sci. Technol. A **3**, 1565 (1985).

12 E. Clementi and C. Roetti, Atomic and Nuclear Data Tables (Academic, New York, 1974), Vol. 14, Nos. 3 and 4.

13 S. M. Foiles, M. I. Baskes, C. F. Melius and M. S. Daw, J. Less-Common Met. **130**, 465 (1987).

14 J. H. Rose, J. R. Smith, F. Guinea, and J. Ferrante, Phys. Rev. B 29, 2963 (1984).

15 A. F. Voter and S. P. Chen, Mater. Res. Soc. Symp.**82**, 175 (1987).

16 D. J. Oh and R. A. Johnson, J. Mater. Res. **3**, 471 (1988) and " Embedded Atom Method for Close-Packed Metals "Atomistic Modelling of Materials: Beyond Pair Potentials" ed. V. Vitek and D. J. Srolovitz , (Plenum to be published) World Materials Congress Proc. 1988

17 G. J. Ackland, G. Tichy, V. Vitek, and M. W. Finnis, Phil. Mag. **56**, 735 (1987).

18 (a) A. F. Voter and J. D. Doll, J. Chem. Phys. **80**,5832 (1984); **82**, 80 (1985); (b) S. M. Valone, A. F. Voter, and J. D. Doll, Surf. Sci. **155**, 687 (1985).

19 (a) For the diffusion of Ni on Ni (110) $[1\bar{1}0]$, see H. P. Bonzel and E. E. Latta, Surf. Sci. **76**, 275 (1978); (b) For Ni/Ni (100), see P. S. Maiya and J. M. Blakely, Appl. Phys. Lett. **7**, 60 (1965)

20 For the low temperature diffusion data for Ni on Ni (110) $[1\bar{1}0]$, see R. T. Tung, W. R. Graham, Surf. Sci. **97**, 73 (1980).

Table I. Arrhenius Parameters

Models	FBD	VC	OJ	ATVF	Expt.
Ni/Ni(100)					
E_a(eV)	0.64	0.71	0.45	0.93	1.54**
D_0(cm^2/s)	0.0038	0.0040	0.0047	0.0074	
Ni/Ni(110)[1$\bar{1}$0]					
E_a(eV)	0.50	0.53	0.44	0.65	0.76*, 1.85**
D_0(cm^2/s)	0.0034	0.0040	0.0038	0.0047	
Ni/Ni(110)[001]					
E_a(eV)	1.30	1.67	1.01	0.65	1.95*, 1.74**
D_0(cm^2/s)	0.0049	0.0082	0.0061	0.0091	

* Table II, ref. 1c, p 230.

** G. Neumann and G. M. Neumann, in Diffusion Monograph Series, "Surface Diffusion of Metals", ed. F. H. Wohlbier, p 54.

Table II. Energetics and geometries

	FBD	VC	OJ	ATVF
Ni/Ni(100)				
Δz (Å)[1]	1.61	1.55	1.72	1.64
$V^{\dagger}$ (eV)[2]	0.64	0.71	0.45	0.94
Ni/Ni(110)[1$\bar{1}$0]				
Δz (Å)[1]	1.11	1.06	1.20	1.14
$V^{\dagger}$ (eV)[2]	0.50	0.53	0.44	0.65
Ni/Ni(110) [001]				
Δz (Å)[1]	1.11	1.06	1.20	1.14
$V^{\dagger}$ (eV)[2]	1.31	1.68	1.02	1.54
Ni/Ni(111)				
Δz (Å)[1]	1.84	1.79	1.94	1.89
$V^{\dagger}$ (eV)[2]	0.06	0.07	0.05	0.05

1. Distance above the surface in the reactant binding site.

2. Classical diffusional barrier.

Figure Captions

Figure 1. Adatom diffusion on (110) [110] as well as on (100) surface together with the mass transfer data.

Figure 2. Directional anisotropy of diffusion on 110 surfaces. The available experimental data at low temperatures refer to the intrinsic surface diffusion.

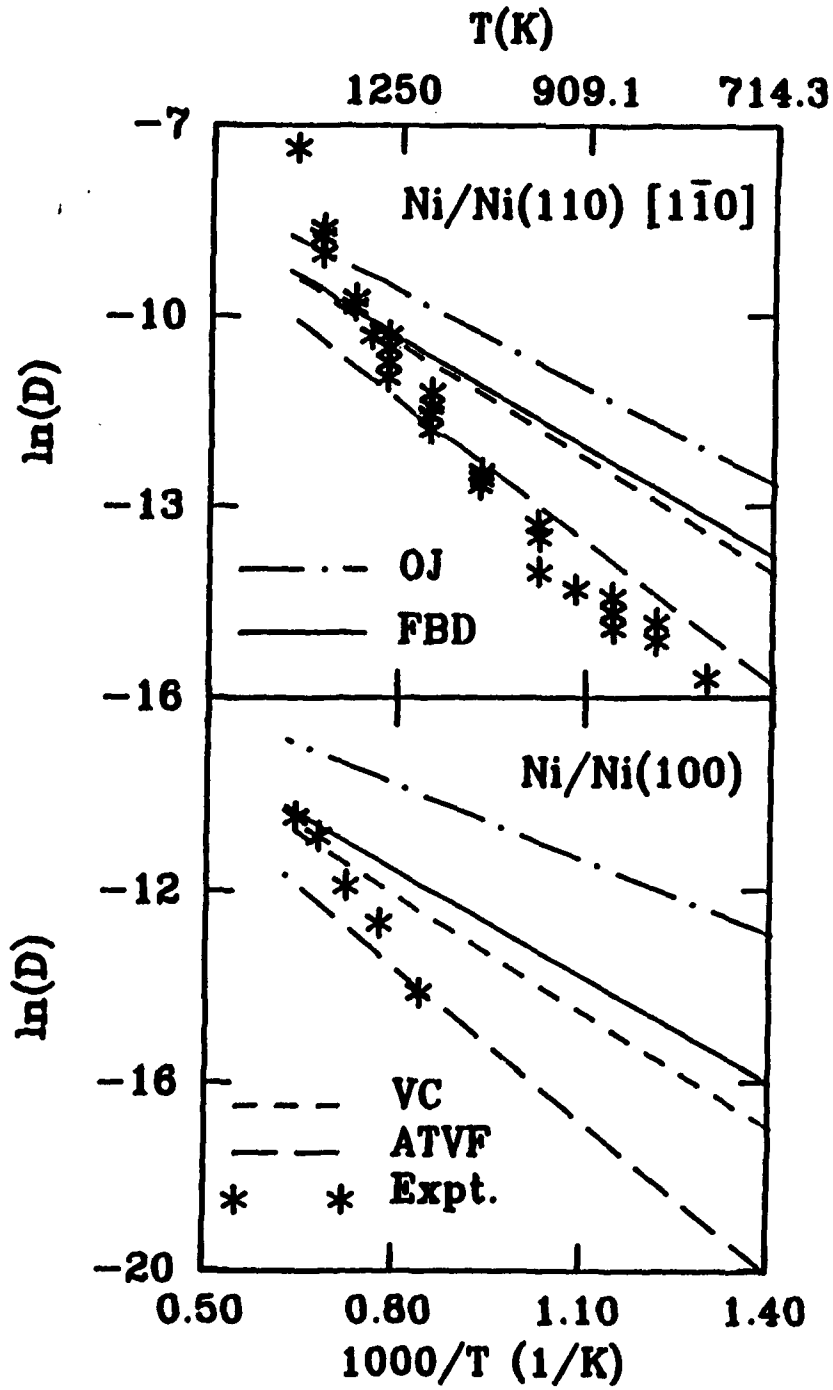
T(K)
1250
909.1
714.3
-7
-10
-13
-16
ln(D)
Ni/Ni(110) [1$\bar{1}$0]
OJ
FBD
Ni/Ni(100)
-12
-16
-20
ln(D)
VC
ATVF
Expt.
0.50
0.80
1.10
1.40
1000/T (1/K)

FIG. 1

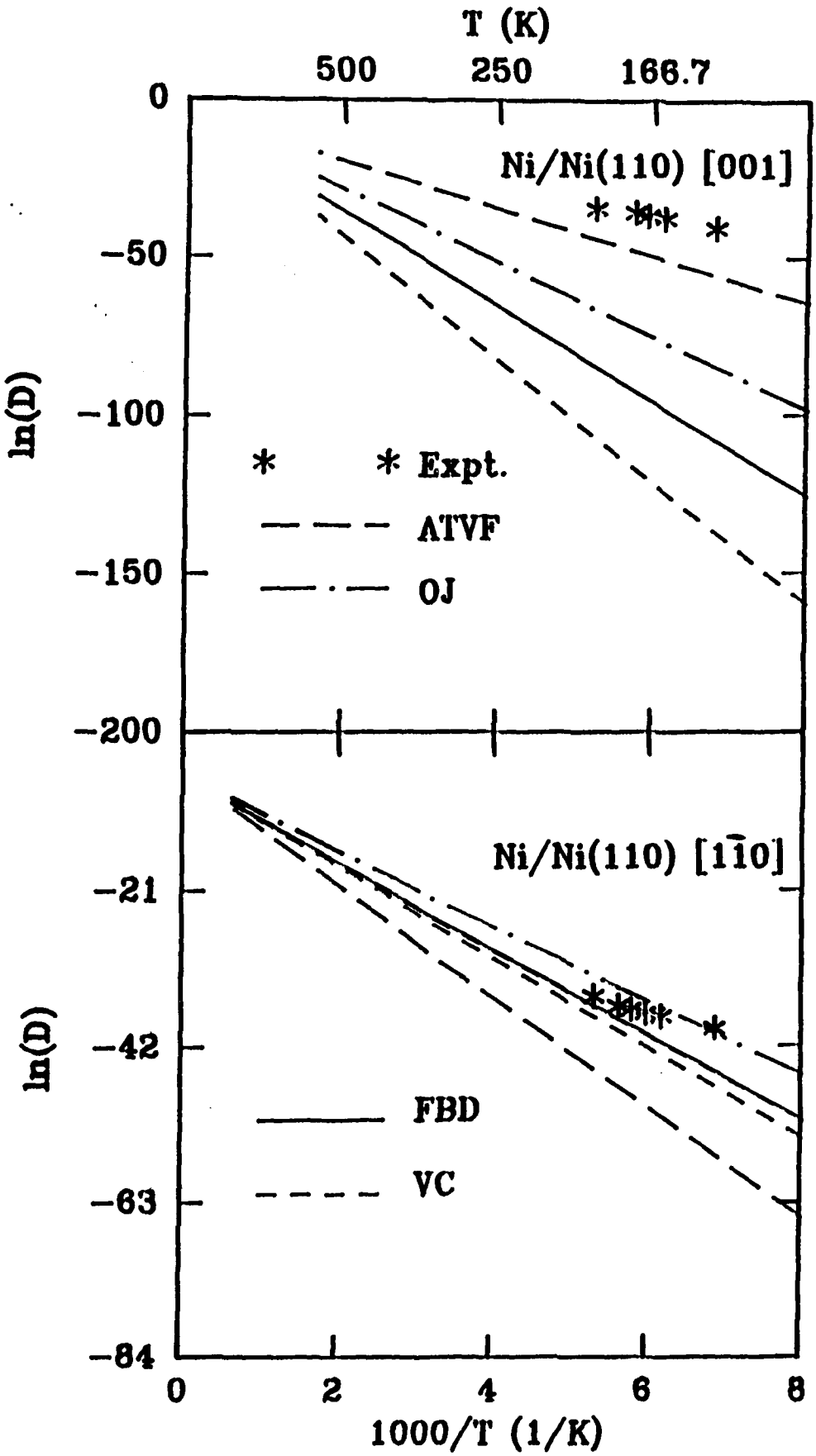
T (K)
500
250
166.7
0
-50
-100
-150
-200
ln(D)
Ni/Ni(110) [001]
* Expt.
ATVF
OJ
-21
-42
-63
-84
Ni/Ni(110) [1$\bar{1}$0]
FBD
VC
0
2
4
6
8
1000/T (1/K)

FIG. 2